AD-A163 785 A STUDY INTO THE MECHANISM(S) FOR THE ELECTROPLASTIC EFFECT IN METALS AND..(U) NORTH CAROLINA STATE UNIV AT RALEIGH DEPT OF MATERIALS ENGINE.. H CONRAD 31 DEC 85 1/1

UNCLASSIFIED ARO-18184.12-MS DAAG29-81-K-0075 F/G 11/6 NL

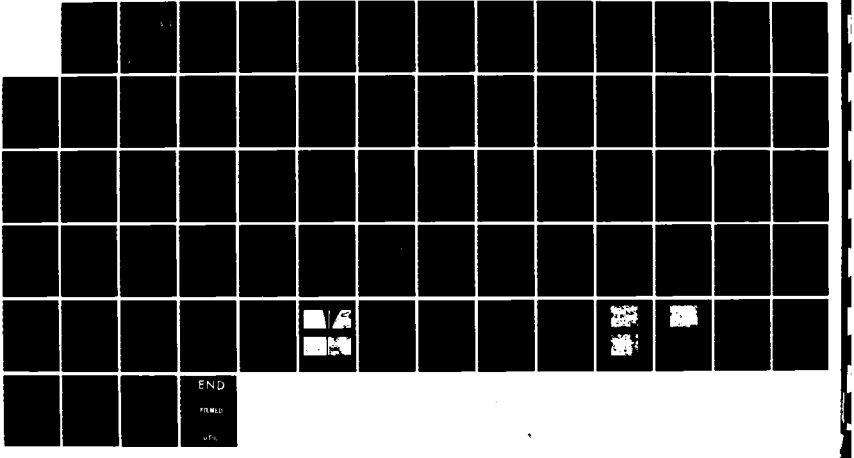

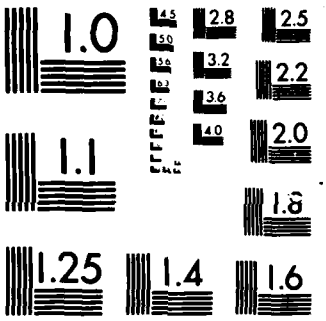

MICROCOPY RESOLUTION TEST CHART
NATIONAL BUREAU OF STANDARDS 1963-A

ARO 18184.12-MS

(2)

A STUDY INTO THE MECHANISM(S) FOR THE ELECTROPLASTIC EFFECT IN METALS AND ITS APPLICATION TO METALWORKING

Final Report

Hans Conrad

December 31, 1985

U.S. Army Research Office

ARO Proposal No. 18184-MS

Research Agreement No. DAAG29-81-K-0075

Materials Engineering Department
North Carolina State University
Raleigh, NC 27695-7901

Approved for Public Release;
Distribution Unlimited

THE VIEW, OPINIONS, AND/OR FINDINGS CONTAINED IN THIS REPORT ARE THOSE OF THE AUTHOR(S) AND SHOULD NOT BE CONSTRUED AS AN OFFICIAL DEPARTMENT OF THE ARMY POSITION, POLICY, OR DECISION, UNLESS SO DESIGNATED BY OTHER DOCUMENTATION.

UNCLASSIFIED
SECURITY CLASSIFICATION OF THIS PAGE (When Data Entered)

REPORT DOCUMENTATION PAGE		READ INSTRUCTIONS BEFORE COMPLETING FORM
1. REPORT NUMBER ARO 18184.12-MS	2. GOVT ACCESSION NO.	3. RECIPIENT'S CATALOG NUMBER
4. TITLE (and Subtitle) A Study Into the Mechanism(s) for the Electroplastic Effect in Metals and Its Application to Metalworking		5. TYPE OF REPORT & PERIOD COVERED Final Report May 1, 1981 to Oct. 31, 1985 6. PERFORMING ORG. REPORT NUMBER
7. AUTHOR(s) Hans Conrad		8. CONTRACT OR GRANT NUMBER(s) 18184-MS DAAG29-81-K-0075
9. PERFORMING ORGANIZATION NAME AND ADDRESS Materials Engineering Department North Carolina State University Raleigh, NC 27695-7907		10. PROGRAM ELEMENT, PROJECT, TASK AREA & WORK UNIT NUMBERS
11. CONTROLLING OFFICE NAME AND ADDRESS U. S. Army Research Office Post Office Box 12211 Research Triangle Park, NC 27709		12. REPORT DATE December 31, 1985 13. NUMBER OF PAGES 68
14. MONITORING AGENCY NAME & ADDRESS(if different from Controlling Office)		15. SECURITY CLASS. (of this report) Unclassified 15a. DECLASSIFICATION/DOWNGRADING SCHEDULE

16. DISTRIBUTION STATEMENT (of this Report)

Approved for public release; distribution unlimited.

17. DISTRIBUTION STATEMENT (of the abstract entered in Block 20, if different from Report)

NA

18. SUPPLEMENTARY NOTES

The view, opinions, and/or findings contained in this report are those of the author(s) and should not be construed as an official Department of the Army position, policy, or decision, unless so designated by other documentation.

19. KEY WORDS (Continue on reverse side if necessary and identify by block number)

Electroplastic, electric current, drift electrons, dislocations, electron drag, electron wind, flow stress, thermally-activated deformation, fatigue life, H-embrittlement, annealing, tempering, sintering, superconductivity, Peierls stress, dislocation kinks.

20. ABSTRACT (Continue on reverse side if necessary and identify by block number)

High density (~10^5 A/cm^2) d.c. current pulses (~100 us) produced a marked decrease in the flow stress of polycrystalline metals (Al, Cu, Ni, Fe, Nb, W, Ti) tested in tension and in the force to draw Cu wire. A significant fraction of the decrease in stress or force could be attributed to drift electron-dislocation interactions, a major component of which was an electron wind with a "push" coefficient of ~10^{-4} dyn-s/cm^2. High density current pulses also

DD FORM 1 JAN 73 1473 EDITION OF 1 NOV 65 IS OBSOLETE

UNCLASSIFIED
SECURITY CLASSIFICATION OF THIS PAGE (When Data Entered)

enhanced the rates of sintering Al powder compacts, the recovery, recrystallization and grain growth of Cu and grain growth in Ti. In addition, the current pulses reduced the annealing twin frequency in Cu and sharpened the grain size distribution in Ti. No significant effect of current pulses on H-embrittlement of Fe at 300K was found.

A continuous d.c. current of 650 A/cm^2 retarded the tempering rate of a hardened tool steel. On the other hand, no changes were noted in the fatigue life of 316 stainless steel for continuous currents of 10 to 100 A/cm^2, nor in the annealing behavior of Cu for currents of 200 to 3100 A/cm^2.

The deformation kinetics of Nb single crystals in the "normal" state were determined over the temperature range of 4.2 to 300K, employing a magnetic field at temperatures below 10K to retain the normal state. The results led to the conclusion that the rate controlling mechanism was thermally-activated overcoming of the Peierls hills by the nucleation and migration of kink-pairs on screw dislocations, the kink-pair energy for Nb being 0.66 ev.

Final Report

ARO Proposal No. 18184-MS: Research Agreement No. DAAG29-81-K-0075

A STUDY INTO THE MECHANISM(S) FOR THE ELECTROPLASTIC EFFECT IN METALS AND ITS APPLICATION TO METALWORKING

Hans Conrad

Materials Engineering Department
North Carolina State University
Raleigh, NC 27695-7901

Contents

Contents (continued)

Final Report

on

ARO Proposal No. 18184-MS: Research Agreement No. DAAG29-81-K-0075

A STUDY INTO THE MECHANISM(S) FOR THE ELECTROPLASTIC EFFECT IN METALS AND ITS APPLICATION TO METALWORKING

Summary

The work performed on this project was in three general categories: (a) effects of high density (~ 10^3 A/mm^2) d.c. pulses, (b) effects of low density (0.1 - 31 A/mm^2) continuous d.c. current and (c) equipment and background information for studying the normal-to-superconducting transition on the flow stress of Nb alloys in relation to the electroplastic effect.

Investigations were carried out into the effects of high density d.c current pulses on the flow stress of metals, wire drawing, the recovery and recrystallization of previously deformed Cu and Ti, sintering of Al compacts and the H-embrittlement of Fe. The various contributions to the drop in flow stress which occurred when a current pulse was applied during a tension test were identified and an analysis of the results indicated that an electron-dislocation interaction occurs in addition to the side effects of the current, such as Joule heating, etc. The electron wind component of this interaction was established to be of the order of 10^{-4} dyne-s/cm^2. An electron-dislocation interaction also contributed to the decrease in force required to draw Cu wire when high density current pulses were applied.

Concurrent application of current pulses during the annealing of cold worked Cu wire enhanced the rates of recovery, recrystallization and grain growth and produced such changes in microstructure as a finer recrystallized grain size, less annealing twins and irregular grain boundaries. In the case

of Ti, there occurred a finer recrystallized grain size and a sharpened distribution of sizes. An increase in the sintering rate of Al powder compacts resulted from the application of current pulses. Current pulsing did not reduce the H-embrittlement of Fe.

The influence of a continuous low density d.c. current on: (a) the fatigue of 316 stainless steel, (b) the recovery and recrystallization of Cu and (c) the tempering of a tool steel were investigated. No significant effect of current densities of 0.1 to 1 A/mm^2 on the fatigue life of 316 stainless steel was found. Likewise current densities of 2 to 31 A/mm^2 had no effect on the recovery or recrystallization of Cu. On the other hand, the tempering rate of a hardened tool steel was significantly retarded by the application of 6.5 A/mm^2 during the tempering process.

A cryostat with a 2 Tesla superconducting magnet and fixtures for tensile testing was designed, purchased and calibrated. The plastic deformation kinetics of Nb in the normal state were determined over the temperature range of 4.2K to 300K in 10-20°K intervals. The results were analyzed using Seeger's theory for the nucleation and spreading of kink-pairs, which yielded $2H_k$ = 0.66 ev, in good accord with the kink energy obtained by others. The present results provide additional support for the concept that the deformation kinetics of BCC metals at low temperatures reflects the overcoming of the Peierls-Nabarro stress by the nucleation of kink-pairs on screw dislocations.

Final Report

on

ARO Proposal No. 18184-MS: Research Agreement No. DAAG29-81-K-0075

A STUDY INTO THE MECHANISM(S) FOR THE ELECTROPLASTIC EFFECT IN METALS AND ITS APPLICATION TO METALWORKING

Introduction

It is now generally accepted that electrons in a metal exert a drag on dislocations, especially those moving at high speeds and at very low temperatures. The electron drag coefficient B_e is given by the following expression

$$(f/\ell) = \tau\, b = B_e v_d \qquad (1)$$

where (f/ℓ) is the force per unit length acting on the dislocation, τ is the resolved shear stress, b the Burgers vector and v_d the dislocation velocity. B_e has been determined for metals by a number of methods, including ultrasonic attenuation, dislocation velocity measurements, and the decrease in flow stress associated with the normal-to-superconducting (n-s) transition, and values in the range of 10^{-6} to 10^{-3} dyne-s/cm^2 have been reported. However, recent considerations (1-4) suggest that B_e is probably of the order of 10^{-5} dyne-s/cm^2. Additional evidence for an interaction between electrons and moving dislocations is provided by the effects of magnetic fields on the flow stress of metals (1,5-7).

Less well known is the idea that drift electrons in a metal may assist dislocations in overcoming obstacles to their motion; i.e. that drift electrons can exert a push or "wind" on dislocations, in contrast to a drag. That drifting electrons in a metal crystal may interact with the dislocations therein was first reported by Troitskii and Likhtman in 1963 (8). They found during electron irradiation of Zn single crystals undergoing plastic deforma-

tion that there occurred a decrease in the flow stress and an improvement in ductility when the electron beam was directed along the (0001) slip plane, compared to when it was normal to the plane. These results were subsequently confirmed by Troitskii (9) and led him to conclude that drift electrons can exert a force ("electron wind") on dislocations, and therefore that such a force should occur during the passage of an electric current through a metal being plastically deformed.

The idea that drift electrons can influence the generation and motion of dislocations led Troitskii and other Soviet scientists to conduct an extensive series of investigations into the influence of direct current pulses of the order of 10^3 A/mm^2 for ~ 50 μs duration on the mechanical properties of metals, including the flow stress (10-15), stress relaxation (16-19), creep (20-22), dislocation generation and mobility (23,24), brittle fracture (25-27), fatigue (28) and metalworking (20,29-38). High current densities were employed to enhance the effect of the drift electrons, short times to reduce Joule heating. The observed effect of the electric current pulses on plastic flow was termed an electroplastic (ep) effect.

Characteristics of the ep effect noted by Troitskii and co-workers in a series of studies on a number of metal single and polycrystals are summarized in Table 1. In this table ΔP is the drop in load (stress) which occurs when a current pulse is applied and P is the total load (stress) acting on the deforming specimen just prior to the current pulse. Some of the benefits reported by Soviet scientists resulting from the application of high density d.c. pulses during metalworking are listed in Table 2. That the electroplastic effect is not restricted to metals deformed at relatively low temperatures is indicated by the results of San Martin and co-workers (39), who found that the creep rate of the intermetallic compound V_3Si at elevated tempera-

tures increased when d.c. current was employed to heat the specimen compared to indirect heating. Further, the creep rate was higher for d.c. heating compared to a.c. heating.

That the mechanical properties of metals may also be influenced by low density electric current has been reported by Silveira and co-workers (40,41). They found that the rate of stress relaxation of polycrystalline Al and Cu near 0.5 T_m increased with the application of a small (1.6 A/mm^2) continuous a.c. or d.c. current, the effect being greater for the d.c. current. The effect decreased as the number of times the relaxation was carried out. Further, they found that the d.c. altered the dislocation arrangement in the Cu specimens; there occurred a partial destruction of the cell structure even in the first relaxation cycle (42). No change in the dislocation structure was noted for Al. The results by Silveira and co-workers are in keeping with earlier observations of Kishkin and Klypin (43), who reported that the creep rate of a number of metals increased with the application of currents as low as 0.15 A/mm^2. Also, Karpenko et al. (28) found that the low-cycle fatigue life of low carbon steel in air, in a 3% NaCl solution and in a gaseous H_2 atmosphere was enhanced by the application of a continuous d.c. current of only 0.07 A/mm^2 during the fatigue test. The largest influence of the electric current was noted for the tests in gaseous H_2.

Theoretical considerations of the force exerted by drift electron on dislocations are given in the papers by Kravchenko (44), Klimov et al. (45) and more recently Roschupkin et al. (46); see Table 3. In these considerations, the force due to drift electrons is proportional to the difference between the drift electron velocity v_e and the dislocation velocity v_d. Further, all three theories indicate that the electron wind force f_{ew}/ℓ is proportional to the current density, i.e.,

$$\tau_{ew} b = K_{ew} J \qquad (2)$$

where τ_{ew} is the stress acting on the dislocation due to an electron wind, b the Burgers vector, K_{ew} the electron wind force factor and J the current density. The theories differ however in the magnitude of the constant K_{ew} and in turn in the value of the electron push (drag) coefficient B_{ew} given by

$$B_{ew} = \tau_{ew} b/v_e = K_{ew} en \qquad (3)$$

where e is the electron charge and n the electron density. The values of B_{ew} predicted by Kravchenko's theory for metals (assuming that the dislocation is temporarily held up at some obstacle) are of the order of 10^{-6} dyne-s/cm^2, those by Klimov et al.'s theory 10^{-6} -10^{-4} dyne-s/cm^2 and those by Roschupkin et al.'s theory 10^{-5} -10^{-3} dyne-s/cm^2. These values are all within the range of those measured experimentally for B_e; however Klimov et al.'s theory gives values in best accord with those most generally accepted (1-4).

Studies in the USA on the electroplastic effect in metals have been carried out by Conrad and co-workers (47-51), Varma and Cornwell (52) and Goldman, Montowidlo and Galligan (53). Varma and Cornwell (52) investigated the effects of current pulses of 250-370 A/mm^2 for several seconds duration on the flow stress of single and polycrystals of Al. The ratio of stress drop $\Delta\sigma_f$ to total flow stress σ_f ranged between 2 to 6% for polycrystalline specimens and 2 to 50% for single crystals, increasing with increase in voltage across the capacitor bank (current density) and with decrease in strain rate in the range of 10^{-3} to 10^{-5} s^{-1}. The effect of strain rate became especially large in single crystals for strain rates below about 3×10^{-5} s^{-1}.

Goldman, Montowidlo and Galligan (53) studied the following two effects on the flow stress of Pb crystals tested at 4.2K: (a) switching on and off

continuous d.c. current (2-8 A/mm^2) and (b) d.c. pulses (1.4-8.0 A/mm^2). At low current densities ($J < \sim 3$ A/mm^2) the specimen was superconducting and no effect of current on the flow stress was detected. At higher current densities the specimen became normal and a drop in stress occurred, which the authors deduced to be due entirely to Joule heating, leading them to the conclusion that no significant electron-dislocation interaction occurred at the low current densities they employed.

Prior to the present study Conrad and co-workers (47-51) had carried out a series of investigations into the effects of single, high density d.c. pulses ($\sim 10^3$ A/mm^2 for ~ 60 μs duration) on the flow stress of a number of polycrystalline metals (Pb, Sn, Fe, and Ti), representing a range in crystal structures and valancies. The objectives of the work were to determine: (a) the magnitude of the drift electron-dislocation interaction which occurs with the application of a current pulse during plastic flow, and (b) the physical basis of the interaction. To arrive at the magnitude of the electron-dislocation interaction, special attention was given to separating out the side effects of the current, such as Joule heating, pinch, skin and magnetostrictive effects.

The early work of Okazaki, Kagawa and Conrad (47-51) focused on the CPH metal Ti. Employing conventional recorders with response times of fractions of a second, it was found that a significant portion ($\sim 1/3$) of the load (stress) drop associated with a current pulse of 5000 A/mm^2 could not be accounted for by the reversible side effects of the current. Moreover, computer calculations indicated that the plastic flow associated with the stress drop could be explained by assuming the existence of an electron-dislocation interaction stress σ_{ed} which added to the applied thermal component of the flow stress σ^* in providing thermally-activated plastic flow. Agreement between the experimental data and the computer calculations occurred when

σ_{ed} was taken to be

$$\sigma_{ed} = C_{ed}J \tag{4}$$

with $C_{ed} = 1.9 \times 10^{-4}$ MPa/(A/cm^2)† for high purity Ti tested at 300K. C_{ed} was found to decrease slightly with increase in strain rate and with decrease in temperature between 300 and 78K; also it increased with interstitial solute content.

Although the proportionality between σ_{ed} and the current density J in Eq. 4 is in accord with the theories for an electron wind effect mentioned above, the value of the constant C_{ed} is 3 to 4 orders of magnitude larger than predicted by these theories, or those observed experimentally for B_e. Thus, in the case of Ti, the fraction of the load drop attributed to an electron-dislocation interaction appears to be due to some effect in addition to an electron wind.

Finally, worthy of mention in relation to the electroplastic effect is that an externally applied electric field may also have an influence on dislocation motion. Klypin and co-workers (54-56) reported increases in the creep rate of metals and alloys at room and elevated temperature upon the application of electric fields of the order of 100 V/cm. Further, electric fields of 103-105 V/cm have been found to increase the rate of dislocation multiplication in rocksalt (57) and the plastic strain rate in ZnSe (58).

In a broader context, the influence of electric fields and currents on the mechanical properties of crystalline solids can be considered to be part of the more general subject of electron-crystal defect interactions, which include their effects on such solid state phenomena as diffusion (electromigration) (59-68) and phase transformations (69-74).

---

†The value of C_{ed} is incorrectly listed as 9.9×10^{-4} MPa/A/cm^2 in Ref. 50.

Results on ARO Project

1. General

The research carried out on this project pertains to the general area of drift electron-crystal defect interactions, with special attention to plastic deformation and solid state transformations. The work was in the following three categories: (a) the effects of high density ($\sim 10^3$ A/mm^2) d.c. pulses, (b) the effects of low density (0.1-31 A/mm^2) continuous d.c. current and (c) the effects of the normal-to-superconducting transition on the flow stress in relation to the electroplastic effect. The following is a list of the activities in each of the three categories of research:

a. High Density d.c. Pulses ($\sim 10^3$ A/mm^2 for $\sim$ 60 μs)

1. Mechanisms for the electroplastic effect in the metals Al, Cu, Ni, Fe, Nb, W and Ti.
2. Effect of repeated current pulses on the drawing of Cu wire.
3. Effect of repeated current pulses on the recovery, recrystallization and grain growth of cold worked Cu and Ti.
4. Effect of repeated current pulses on H-embrittlement of Fe.
5. Effect of repeated current pulses on the sintering of Al powder.

b. Low Density Continuous d.c. Current (0.1-31 A/mm^2)

1. Effect on fatigue of 316 stainless steel.
2. Effect on recovery, recrystallization and grain growth in Cu.
3. Effect on the tempering of steel.

c. Normal-to-Superconducting Transition

1. Designed, purchased and calibrated a cryostat with superconducting magnet (2 Tesla) and fixtures for tension tests in the range of 1.2 to 300K.

2. Determined the deformation kinetics of high purity Nb in the normal state from 4.2 to 300K.

Most of the effort concentrated on the mechanisms for the electroplastic effect in metals, i.e. on the nature of the electron-dislocation interaction which occurs during the application of a single, high density d.c. current pulse. The other studies on the effects of electric current were more exploratory in nature, since little, if any, work had been previously carried out on these subjects. The work on the n-s transition experienced some delay because of the time required to design, acquire and get into operation the cryostat with superconducting magnet. The papers published or submitted on the project are presented in Table 4. The results in papers I-4, I-5 and II-3 provide background information important to evaluating the influence of electric current on the plastic flow of Ti and on the recovery and recrystallization of this metal.

The theses completed by students working on the project are listed in Table 5.

2. Effects of High Density d.c. Current Pulses

a. Mechanisms for the Electroplastic Effect: As mentioned above, most of the effort focused on this topic. The results obtained are presented in detail in papers I-1, I-2, I-3 listed in Table 4 (Refs. 75-77 at end of this report). The following is a summary of the results obtained in this study.

The effects of high density d.c. current pulses ($\sim 10^3$ A/mm^2 for 60 μs) on the flow stress of a number of polycrystalline metal wires (Al, Cu, Ni, Fe, Nb, W and Ti) representing a range in crystal structure, stacking fault energy and electronic structure were investigated using high speed recording equipment. Good agreement was obtained between the measured temperature rise due

to Joule heating resulting from the current pulse and that: (a) calculated assuming adiabatic conditions and (b) deduced from the associated thermal expansion. Because of test machine inertia, a delay time of ~ 2 ms occurred before the machine responded to the specimen elongation produced by the current pulse. The resulting oscillations in the load signal were electronically filtered with a 10 Hz low-pass filter, so that the maximum drop in the load (stress drop $\Delta\sigma_f$) was recorded at ~ 50 ms.

Both reversible, $\Delta\varepsilon_E$, and irreversible (plastic), $\Delta\varepsilon_p$, strains contributed to the measured stress drop $\Delta\sigma_f$ which occurred upon application of a current pulse. $\Delta\sigma_f$ increased with increase in current density J and amounted to as much as 36% of the prior flow stress σ_f. The major component of $\Delta\varepsilon_E$ was thermal expansion due to the Joule heating; other side effects of the current such as skin, pinch and magnetostrictive effects were much smaller in magnitude. Assuming that the measured load drop was that which occurred at the end of the current pulse, computer calculations indicated that thermally-activated plastic flow due to the Joule heating (i.e., thermal softening) made a negligibly small contribution to $\Delta\varepsilon_p$, leading to the conclusion that $\Delta\varepsilon_p$ was mainly due to some electron-dislocation interaction, $\Delta\varepsilon_{ed}$.

The magnitude of $\Delta\varepsilon_p$ decreased with the amount of prior plastic deformation for the FCC metals Al and Cu, but was relatively independent of strain ε for the BCC metals and CPH Ti; see Fig. 1. This effect of ε on $\Delta\varepsilon_p$ is in accord with the concept that the drift electrons help the mobile dislocations overcome the obstacles generally accepted to be rate-controlling in these three classes of metals, namely intersection of forest dislocations, overcoming of the Peierls-Nabarro stress and overcoming interstitial solute atoms, respectively. The effect of ε on $\Delta\varepsilon_p$ for the FCC metal Ni was irregular, which was attributed to possible dynamic strain aging effects.

The thermally-activated dislocation motion concept was employed to determine the mechanisms by which the drift electrons might enhance the dislocation mobility and thereby yield $\Delta\varepsilon_{ed}$.† The plastic strain rate $\dot{\varepsilon}$ was assumed to be given by the Arrhenius-type rate equation

$$\dot{\varepsilon} = \dot{\varepsilon}_o \exp(-\Delta H^*(\sigma^*)/kT) \tag{4}$$

where $\dot{\varepsilon}_o$ is the pre-exponential factor and includes the activation entropy, and ΔH^* is the activation enthalpy, which is a decreasing function of the effective stress σ^*. Expanding $\Delta H^*(\sigma^*)$ to

$$\Delta H^*(\sigma^*) = \Delta H^* - v^* \sigma^* \tag{5}$$

where v^* is the so-called activation volume, one obtains for a current pulse:

$$\ell n(\dot{\varepsilon}_{ed}/\dot{\varepsilon}_i) = \ell n\,(\dot{\varepsilon}_{o_{ed}}/\dot{\varepsilon}_o) - \frac{(\Delta H^*_{ed} - \Delta H^*)}{kT} + \frac{(v^*_{ed} - v^*)\sigma^*}{kT} + \frac{v^*_{ed}\sigma_{ew}}{kT} \tag{6}$$

In Eq. 6 the subscript ed refers to the values of the various parameters associated with the current pulse and σ_{ew} is the electron wind stress acting on the dislocations temporarily held up at their respective obstacles. $\dot{\varepsilon}_i$ is the plastic strain rate prior to the application of the current pulse and $\dot{\varepsilon}_{ed}$(= $\Delta\varepsilon_p$/60 μs) is that resulting from the action of the drift electrons.

For FCC metals we have for the effect of ε on v^* (78)

$$v^* \simeq kT/\sigma m \tag{7}$$

---

†This was considered to be reasonable, since the maximum plastic strain rate during the stress drop was deduced to be < $10^1 s^{-1}$, and therefore in the quasi-static range.

where $m = \partial \ell n \sigma / \partial \ell n \dot{\varepsilon}$ is relatively independent of ε and σ the total applied stress, which increases with ε. Hence, if $\dot{\varepsilon}_{o_{ed}}/\dot{\varepsilon}_i$, $(\Delta H^*_{ed} - \Delta H^*)$ and $(v^*_{ed} - v^*)$ do not vary with ε, Eq. 7 reduces to

$$\ell n \, (\dot{\varepsilon}_{ed}/\dot{\varepsilon}_i) = \alpha + \beta/\sigma \tag{8}$$

where α is a constant representing the first three terms on the RHS of Eq. 6 and $\beta = \sigma_{ew}/m$. Thus, knowing the value of m, one can obtain σ_{ew} as a function of J, and in turn B_{ew} from the relation

$$B_{ew} = \frac{\sigma_{ew} b \, en}{J \, \mathfrak{M}} \tag{9}$$

where e is the electron charge, n the electron concentration and $\mathfrak{M}$ the Taylor orientation factor relating the tensile stress σ to the resolved shear stress τ.

In the case of the FCC metals Al and Cu, σ_{ew} was proportional to J (Fig. 2) and the values of B_{ew} obtained using Eq. 9 were of the order of 10^{-4} dyne-s/cm^2, in reasonable accord with Roschupkin et al.'s (46) theory for an electron wind force acting on mobile dislocations temporarily held up at obstacles; see Table 3. This value of B_{ew} is in accord with the dislocation damping constant B determined by other techniques at 300K (Figs. 3 and 4), which is thought however to be due mainly to phonon drag (1-4). It is an order of magnitude larger than recent considerations (1-4) suggest for the electron drag coefficient B_e. As a possible explanation for this difference, it is suggested that the drift electrons may produce a local phonon flux, which exerts a force on the dislocations before it looses its directional character from collisions with the lattice phonons.

In addition to the electron wind effect given by the parameter β of Eq. 8, the current pulse had an effect on α, which increased with J^2 for Al and Cu

(Fig. 5). Since α includes at least six components ($\dot{\varepsilon}$, $\dot{\varepsilon}_{o_{ed}}$, ΔH^*, ΔH^*_{ed}, v^*, v^*_{ed}) the mechanism for the effect of J on α could not be uniquely identified.

The values of $\Delta\varepsilon_p$ for the BCC metals were similar in magnitude to those of the FCC metals, suggesting the occurrence of a significant electron-dislocation interaction for this class of metals as well. However, the electron wind force could not be separated from the other drift electron contributions in the manner of the FCC metals, because $\Delta\varepsilon_p$ did not vary with ε. In the case of CPH Ti, $\Delta\varepsilon_p$ was significantly higher than than for the other metals, in accord with the higher drift electron velocity in this metal.

Taking machine inertia effects into account, it was found that the magnitude of $\Delta\varepsilon_p$ was smaller than when they were neglected, but the general conclusions deduced therefrom were similar. The calculations based on the inertia effect could only be considered to be approximate, because of the small strains involved ($\Delta\varepsilon_p \approx 10^{-4}$) and the limited accuracy of the thermal activation functions and parameters employed in the analysis.

b. Application of the Electroplastic Effect to Wire Drawing: To investigate the application of the ep effect to metalworking, d.c. pulses of 3000 to 9000 A/mm^2 and 108 μs duration were applied at frequencies of 20 and 50 Hz during the drawing (22% R.A.) of Cu wire surrounded by a silicone oil bath at 300K using an Instron machine operating at a crosshead speed of 4.2×10^{-2} mm/s. The experimental arrangement is shown in Fig. 6. The drawing force decreased upon application of the current pulses; see, for example, Fig. 7. The drop in the drawing force ΔP ranged from 1 to 14% of the force P_0 without current and increased linearily with J for both pulsing frequencies; see Fig. 8.

Both Joule heating and electron-dislocation interaction effects are expected to contribute to the decrease in drawing force produced by the cur-

rent pulsing. The temperature rise was measured by an iron-constantan thermocouple (0.07 mm dia.) spot welded to the Cu wire just prior to its entrance into the die; see Fig. 6. A plot of the load drop ΔP versus the measured temperature rise ΔT for the two pulsing frequencies (f_p) is given in Fig. 9. To be noted is that for the same temperature rise, ΔP increases with f_p, indicating an effect of the current pulses on ΔP in addition to Joule heating. The increase in ΔP with f_p is in keeping with an electron-dislocation interaction, because at the higher f_p the current is flowing a larger fraction of the time. Additional work is needed to better resolve the various contributions to the reduction in the drawing force.

No polarity effects of the d.c. electric current on the drawing force were noted in the present experiments. This differs from the findings of Troitskii and co-workers (37) for the drawing of Cu wire at somewhat higher speeds and pulsing frequencies, who found a significantly larger effect when the (+) terminal was upstream of the die compared to when the (-) terminal was at this location (37).

c. Effects of Repeated Current Pulses on Recovery, Recrystallization and Grain Growth: The effects of repeated current pulses ($J = 800$ A/mm^2, $t_p = 100$ μs, $f_p = 2$ Hz) on the isochronal annealing behavior of tough pitch Cu and 99.97% Ti were investigated. The results on Cu have been published and are presented in Refs. 92 and 93.

An example of the results on Cu is presented in Fig. 10. Evident in the upper portion of the figure are the increased rates of recovery and recrystallization which resulted from the application of the current pulses.† The

† The maximum temperature rise which occurred as a result of the pulsing was 3°C.

lower portion of the figure shows the effect of the current pulses on the recrystallized microstructure, the current pulsing having produced less sharply defined grain boundaries (and generally more irregular) and a lower density of annealing twins. Also, it was found that the initial recrystallized grain size was finer in the pulsed specimens; however, the rate of subsequent grain growth was higher. These effects of current pulsing on annealing behavior of Cu were found to decrease as the amount of prior cold work was increased in the range of 24% to 76% R.A. (93).

It was proposed that the higher mobility of dislocations produced by the electric current was in part responsible for many of the effects observed during the annealing of Cu, either directly or indirectly. The increased rate of recovery can be attributed to increased rates of annihilation of positive and negative dislocations due to enhanced glide, cross slip and climb. Further, the fact that the influence of the current pulses on the recrystallization temperature and recrystallized grain size decreases with degree of prior cold work suggests that the electric current assists the process of subgrain coalescences needed to achieve the required misorientation for sustained growth of a subgrain into a strain-free grain. As the degree of cold work is increased, less subgrain coalescence is needed to achieve the required misorientation (15° - 20°) for a subgrain to grow into a strain-free new grain and therefore the smaller is the effect of the current pulses. In regard to the reduced twinning frequency, it is proposed that the current pulses promote irregular growth of the grains, which disturbs the interfacial equilibrium conditions needed for annealing twin formation. The enhanced rate of grain growth may be due to: (a) the greater irregularity of the grain boundaries in the pulsed samples, giving smaller radii of curvature and a

larger grain boundary area per unit volume, both leading to an increase in driving force and (b) an enhanced atomic mobility at the grain boundaries due to electromigration effects.

Results obtained in the study into the effects of current pulsing during the annealing of cold worked Ti (50% reduction in area by wire drawing) are presented in Figs. 11-14. Figure 11 shows that no significant change in hardness occurred as a result of the current pulsing when corrections are made for the increase in temperature ($\Delta T \simeq 70^{0}C$) associated with the current pulses. Metallographic examination of fully recrystallized specimens however revealed that for a given annealing temperature the grain size of the pulsed specimens was smaller than that of specimens annealed without current pulsing; see Fig. 12. Further, the grain size distribution tended to be somewhat sharper in the current pulsed specimens, Figs. 13 and 14. The finer grain size produced by current pulsing is in accord with the results for Cu, but the lack of a change in hardness during recovery and early recrystallization differs from the behavior of Cu. The difference in behavior between Ti and Cu indicates that the processes of recovery and of the nucleation of new grains (94-97) are not influenced by the current to the same degree in Ti as in the Cu.

d. Effect of Repeated Current Pulses on Hydrogen Embrittlement in Fe: To investigate the possibility of an interaction between electrons and hydrogen in a metal being deformed, current pulses ($J = 2500\ A/mm^2$, $t_p = 108\ \mu s$, $f_p = 2\ Hz$) were applied during the tensile deformation ($\dot{\varepsilon} = 1.7 \times 10^{-4}\ s^{-1}$ and $T = 300K$) of Fe specimens (99.9% purity, annealed for 45 min. at 800°C) charged with H. Charging with H for 2 hrs. reduced the tensile elongation from 21.7% to 1.9% in specimens tested without current pulses. Upon application of the current

pulses, the elongation of an uncharged specimen became 17.6%, whereas that of a H-charged specimen was 0.9%. Thus, the current pulsing did not reduce the embrittling effect of the H-charging. A decrease in elongation (21.7% to 17.6%) experienced by the uncharged specimens as a result of the current pulsing was attributed to the temperature rise ($\Delta T = 24^{o}C$) from the Joule heating associated with the current pulsing, since a similar loss in ductility occurred when an uncharged specimen was heated indirectly by hot air during the tensile test. Similarily, the decrease in elongation of the H-charged specimen from 1.9% to 0.9% resulting from the current pulsing may be due to the temperature rise associated with the pulsing.

e. Effect of Repeated Current Pulses on the Sintering of Al Powder: The results of preliminary experiments suggest that enhanced sintering occurs when current pulses ($J = 1400$ A/mm^2, $t_p = 85$ μs, $f_p = 6$ Hz) were applied for 30 minutes to cold isostatically-compacted (300-500 MPa) commercial 00010 Al powder (325 mesh) specimens initially at 300K. The Joule heating due to the current pulses produced a temperature rise of $\sim 250^{o}C$. However, the degree of densification was greater than resulted from simply heating the specimen to this temperature. This is in accord with the enhanced sintering which occurred upon application of an a.c. electric current by Lenel (98) during hot pressing of metal powders.

3. Effects of Low Density Continuous d.c. Current

a. Fatigue of 316 Stainless Steel: Studies were conducted on the effect of low density (0.1-10 A/mm^2) continuous d.c. current on the fatigue life of 316 stainless steel tested in rotating bending at 300K. Interest in this subject was stimulated by the work of Karpenko et al. (28), who reported that the low-

cycle life of low carbon steel in air was enhanced by the application of a continuous d.c. current of only 0.07 A/mm^2 during the fatigue test. 316 stainless steel was chosen for these tests, since other fatigue studies (99) are underway on this material.

The results obtained in this study are presented in Figs. 15-17. Although preliminary results (100) suggested that a slight increase in low cycle fatigue life occurred from the concurrent passage of 0.1 A/mm^2 continuous d.c. current during a rotating bending fatigue test, subsequent, more detailed, studies indicated that no effect could be detected outside the scatter in the data; see Fig. 15. Further, no difference in the fracture surface morphology was detected between specimens fatigue tested with current compared to without current, see Fig. 16. The increase in temperature due to the passage of 0.1 A/mm^2 was measured to be 0.12°C.

To enhance any possible effect of an electric current on fatigue life, a second set of tests were conducted in which the current density applied during the fatigue test was increased by an order of magnitude, i.e. to J = 1 A/mm^2. The temperature rise due to Joule heating was now measured to be 12°C. The results of the tests with J = 1 A/mm^2 are presented in Fig. 17. Also included are the results for one specimen tested without current, but heated by forced hot air to the same temperature (ΔT = 12°C) as that produced by Joule heating in the specimen tested with current.

The data of Fig. 17 suggest a decrease in fatigue life as a result of the concurrent application of 1 A/mm^2. However, the lower fatigue life with current is probably due to Joule heating, since the fatigue life of 316 stainless steel decreases with increase in temperature in the vicinity of room temperature (101). The lower fatigue life of the externally heated specimen supports this interpretation.

Thus, the present study indicates that the concurrent application of a d.c. current of the order of 0.1 to 1.0 A/mm^2 during fatigue testing in rotating bending has no significant effect on the fatigue life of 316 stainless steel other than that which may be associated with any temperature rise due to Joule heating. This differs from to the results reported by Karpenko et al. (28) for low carbon steel.

b. Recovery, Recrystallization and Grain Growth in Cu: Cold worked (22% and 76% R.A.) Cu wire specimens were isochronally (15 min) annealed at temperatures in the range of 250°C to 400°C with, and without being subjected to a continuous d.c. current of 2, 10 and 31 A/mm^2. Vickers hardness measurements were made on both sets of the annealed specimens over the entire temperature range considered and grain size distribution measurements were made for the anneals at 305°C, 350°C and 380°C. No effect of the d.c. current was found for either the hardness, (see for example Figs. 18 and 19), or the recrystallized grain size and its distribution. This differs from the behavior noted by Silveira et al. (102), who reported that the concurrent application of a continuous d.c. current in the range of 6.5 to 15.5 A/mm^2 produced a decrease in the grain size of their Cu annealed at 673K.

c. Tempering of Steel: The effect of continuous d.c. current of 6.5 A/mm^2 on the tempering of a quenched AISI (02) tool steel (0.9%C, 1.6%Mn, 0.25%Si) was investigated. The results are presented in Fig. 20. The temperature for the tests with the current includes that due to Joule heating ($\Delta T \approx 20^0$C). To be noted is that a higher temperature is required to attain the same hardness when the current is applied. Of interest is whether this shift to higher temperatures is due to a retardation of tempering kinetics or to a change in

morphology of the microstructure leading to a higher hardness for a given time and temperature of tempering. Optical microscopy was employed as a preliminary attempt to separate these effects.

Figure 21 shows the microstructures obtained with, and without, current for a constant tempering treatment of 30 min at ~ 600K. Careful examination of the photomicrographs, and especially of the specimens directly under the microscope, indicated that the specimen tempered with current contained less tempered martinsite (i.e. had a smaller amount of the darker tempered martinsite structure) than the one without current. A similar trend was noted for specimens tempered at ~ 750K. On the other hand, no clear difference in microstructure could be ascertained for specimens tempered with, and without, current to the same hardness level; see Fig. 22. Thus, the major effect of the current appears to have been to retard the tempering reaction. This differs from the results of Erdmann-Jesnitzer et al. (103,104), who found that a d.c. current accelerated both quench aging and strain aging in a low carbon iron. However, the present conclusion based on optical microscopy can only be considered as tentative, in view of the fineness of the microstructure of the tempered martinsite. Higher resolution of the microstructure by SEM or TEM is needed to more clearly identify the effects of the current during tempering.

4. Normal-to-Superconducting Transition: The objectives of this activity were twofold: (a) to determine the electron drag coefficient B_e from the drop in flow stress which results upon passing through the n-s transition (105-113) and (b) to compare the effects of high density current pulses applied during plastic deformation in the superconducting state with those in the normal state. Both sets of experiments should provide additional information on the nature of electron-dislocation interactions which may occur during the plastic

deformation of metals. Special attention was to be given to repeating the experiments of Goldman et al. (53), but at current densities several orders of magnitude higher than they employed. The materials being considered are Nb and Nb-Mo (1, 2, 6 and 10% Mo) alloys. This alloy system was chosen because of its relatively high transition temperature (9.2K) and because some results on the n-s effect are available for comparison (105-107).

Accomplishments to date on this research activity include: (a) design, purchase and calibration of a cryostat containing a 2 Tesla superconducting magnet and mechanical test fixtures and (b) determining the deformation kinetics of Nb in the normal state from 300 to 4.2K in 10°-20°K intervals. The results of the deformation kinetics provide the background information needed for comparison with the behavior in the superconducting state and for evaluation of the results obtained upon application of high density current pulses.

a. Deformation Kinetics of Nb Single Crystals at Low Temperatures: The deformation kinetics results obtained in uniaxial tension on high purity Nb (99.99%, $\rho_{300}/\rho_{4.2} = \sim 300$) provided by Case Western University (Drs. J. Talia and R. Gibala) are presented in Figs. 23-25. The effect of temperature on the flow stress τ_f (resolved yield stress) and on its thermal τ^* and athermal τ_μ components is given in Fig. 23. The flow stress value at 4.2K was obtained for the normal state by applying a magnetic field H > 2.6 Koe during the tensile test. Brittle behavior at temperatures below 77K was avoided by first straining the specimen a small amount at 77K before continuing the test at the lower temperature. The slight increase in stress due to strain handening at the prior test temperature was subtracted from the flow stress following the temperature change to give the yield stress τ_f at the lower temperature. The

strong temperature dependence of τ_f and τ^* indicated in Fig. 23 was obtained in this manner and is in keeping with that for Nb and other BCC metals (78,114-117). τ_μ was here obtained by the decremental unloading technique (118).

The variation of activation volume

$$v = kT(\partial \ln \dot{\gamma}/\partial\tau)_T \tag{10}$$

with temperature is presented in Fig. 24. $\dot{\gamma}$ denotes the resolved shear strain rate. To be noted in Fig. 24 is that there is good agreement between the two methods employed to determine v.

The deformation kinetics of the Nb crystals were analyzed employing the thermally activated plastic deformation rate equation

$$\dot{\gamma} = \dot{\gamma}_0 \exp(-\Delta G(\tau^*)/kT) \tag{11}$$

where $\dot{\gamma}_0$ is the pre-exponential factor and $\Delta G = \Delta H^* - T\Delta S^*$ is the Gibbs free energy of activation, which is a decreasing function of τ^* ($= \tau - \tau_\mu$). The activation enthalpy ΔH^* is given by (119)

$$\Delta H^* = - vT(\partial\tau^*/\partial T)\,\dot{\gamma} \tag{12}$$

and ΔG by (120)

$$\Delta G = \frac{\Delta H - \alpha v\tau_f}{1 + \alpha} = \frac{\Delta H^* - \alpha v\tau^*}{1 + \alpha} \tag{13}$$

where $\Delta H = - vT(\partial\tau_f/\partial T)_{\dot{\gamma}}$, $\alpha = -(T/\mu)\, d\mu/dT$ and $\mu = \{C_{44}(C_{11} - C_{12}/2\}^{1/2}$ the appropriate shear modulus (121). The variation of ΔH^* and ΔG with temperature obtained using Eqs. 12 and 13 for a constant tensile strain rate of 1.66×10^{-4} s^{-1} is presented in Fig. 25. To be noted is that the data points for ΔG fit well to a straight line passing through the origin (T = 0K), in keeping with Eq. 11. The value of $\dot{\gamma}_0$ derived from the slope of the straight line for

ΔG versus temperature and taking $\dot{\gamma} = 2\dot{\varepsilon}$ is 1.5×10^7 s^{-1}. The values of ΔH^* and ΔG at T = 300K (τ^* = 5 MPa) are 0.68 ev and 0.64 ev respectively. The deformation kinetics results in Figs. 23-25 are in reasonable accord with those reported by others (114-117) for Nb.

It has been proposed (78,117,122-124) that the deformation kinetics of BCC metals at low temperatures ($T < 0.2\ T_m$) reflects the thermally activated overcoming of the Peierls-Nabarro stress by the nucleation and spreading of kinks over the Peierls hills. A detailed theory for this process has been developed by Seeger (117,125), which deals with the formation of kink pairs on screw dislocations. Two models are employed to calculate the enthalpy for the kink-pair formation, depending on the value of the effective stress τ^*. At small τ^*, Regime (i), the stress dependence of the kink-pair formation enthalpy is determined by the elastic interaction of the kinks and therefore the model for this regime is referred to as the elastic interaction (E.I.) approximation. At large τ^*, Regime (ii), the stress dependence is derived from the line-tension model of a dislocation and this regime is referred to as the line-tension (L.T.) approximation. At the strain rates normally employed (10^{-2} to 10^{-4} s^{-1}), Regime (i) consists of two regions: (a) a lower temperature region where kink mobility is not strongly temperature dependent and (b) a higher temperature region where τ^* is very small and kink mobility is strongly dependent on temperature. In the former region, the kink diffusion coefficient is neglected so that the results are the same as for the transition state theory and the approach is termed the transition state (T.S.) approximation. In the higher temperature region, the kink diffusion coefficient is included, and this limiting case is termed the diffusion (Diff.) approximation. Equations for the various regimes derived by Seeger for comparison with experimental data are summarized in Table 6.

peratures ($T < 0.2\ T_m$) reflects an inherent resistance of the BCC lattice to the motion of dislocations on the active slip plane and that the rate-controlling mechanism is the formation and spreading of kink-pairs.

Theoretical calculations of the kink energy based on realistic atom potentials have so far not been made for Nb. They have however been made for BCC α-iron (130,134), whose experimental values of $2H_k$ are similar in magnitude to those for Nb (78,122,124). The theoretical estimates of $2H_k$ for α-iron are included in Table 8. They tend to be higher than those measured; however the most recent value (0.74 ev) by Duesbery (134) can be considered to be in reasonable agreement with the experimental value 0.65 ± 0.05 for Nb.

Acknowledgements

The author (H.C.) wishes to acknowledge the invaluable assistance of Dr. S.L. Mannan, visiting research associate (1982-84) from the Reactor Research Centre, Kalpakkam, Tamil Nadu, India and of Dr. A.F. Sprecher, research associate NCSU (1984-85) in carrying out various phases of this research program. Also, he wishes to express his appreciation to Texaco Corporation for providing graduate fellowships to Mr. A.F. Sprecher and Mr. J. White in support of their graduate program, which included thesis research related to subject matter of this project. Further, the author wishes to recognize the following students, who participated in this research project:

A. Graduate Students

1. A.F. Sprecher, Ph.D. 1984
2. N.H. Karam, Ph.D. 1985
3. S.K. Mannan, M.S. 1985
4. S. Shamala, M.S. anticipated 1986
5. J. White, M.S. anticipated 1986

B. Undergraduate Students

1. S. Hovis, B.S 1983
2. J. Shuping, B.S. 1983
3. L. Hager Kirkpatric, B.S. 1984
4. G. Service, B.S. 1984
5. D. Gandy, B.S. 1984
6. R. Morton, B.S. 1984
7. M. Shurling, B.S. 1984
8. V. Langley, B.S. 1985
9. E. Foster, B.S. anticipated 1986
10. P. Watkins, B.S. anticipated 1986

C. Other Students

1. S. Ricks (NCSU Work-Study)
2. A. Copeland (N.C. School of Science and Math)

References

1. J.M. Galligan, Scripta Met. 18 643, 653 (1984).
2. T. Vreeland, ibid. 18 645 (1984).
3. C. Elbaum, ibid. 18 657 (1984).
4. A.V. Granato, ibid. 18 663 (1984).
5. J.M. Galligan, T.H. Lin and C.S. Pang, Phys. Rev. Letters 38 405 (1977).
6. J.M. Galligan and C.S. Pang, J. Appl. Phys. 50 6253 (1979).
7. L.R. Motowidlo, P.D. Goldman and J.M. Galligan, Scripta Met. 15 787 (1981).
8. O.A. Troitskii and V.I. Likhtman, Kokl. Akad. Nauk. SSSR 148 332 (1963).
9. O.A. Troitskii, Radiation-Induced Changes in the Strength and Plasticity of Zinc Single Crystals, [in Russian], Moscow (1968).
10. O.A. Troitskii, Zh ETF Pis. Red. 10 18 (1969).
11. O.A. Troitskii and A.G. Rozno, Fizika Tverdogo Tela 12 203 (1970).
12. O.A. Troitskii, Fiz. Metal. Metalloved. 32 408 (1971).
13. O.A. Troitskii, Problemy Prochnosty, p. 14 (July 1975).
14. V.I. Spitsyn and O.A. Troitskii, Dokl. Akad. Nauk. SSSR 220 1070 (1975).
15. O.A. Troitskii, Fiziko-Khimichskaya Mekhanika Materialov 13 46 (1977).
16. O.A. Troitskii, V.I. Spitsyn, V.I. Stashenko, Dokl. Akad. Nauk. SSSR 241 349 (1978).
17. O.A. Troitskii and V.I. Stashenko, Fiz. Metal. Metalloved. 47 180 (1979).
18. O.A. Troitskii, V.I. Spitsyn and P.U. Kalymbetov, Dokl. Akad. Nauk. SSSR 253 96 (1980).
19. O.A. Troitskii, P.V. Kalymbetov, Fiz. Metal. Metalloved. 51 1059 (1981).
20. O.A. Troitskii and V.I. Stashenko, Fiz. Metal. Metalloved. 51 219 (1981).
21. O.A. Troitskii, V.I. Stashenko and V.I. Spitsyn, Izv. Akad. Nauk. SSSR Metallii 1 164 (1982).
22. V.I. Stashenko, O.A. Troitskii and V.I. Spitsyn, Phys. Stat. Sol. (a) 79 549 (1983).
23. L.B. Zuev, V.E. Gromov, V.F. Kurilov and L.I. Gurevich, Dokl. Akad. Nauk. SSSR 239 84 (1978).
24. Yu. I. Boiko, Ya. E. Geguzin and Yu. I. Klinchuk, Pis'ma Zh. Eksp. Teor. Fiz. 30 168 (1979).
25. V.I. Spitsyn, O.A. Troitskii and P. Ya. Glazunov, Dokl. Akad. Nauk. SSSR 199 810 (1971).
26. O.A. Troitskii, I.L. Skobtsov and A.V. Men'shikh, Fiz. Metal. Metalloved. 33 392 (1972).
27. Yu. I. Golovin, V.M. Finkel and A.A. Sletkov, Problemy Prochnosty 2 86 (1977).
28. G.V. Karpenko, O.A. Kuzin, V.I. Tkachev and V.P. Rudenko, Dokl. Akad. Nauk. SSSR 227 85 (1976).
29. V.I. Spitsyn, O.A. Troitskii, E.V. Gusev and V.K. Kurdiukov, Izv. Akad. Nauk. SSSR Ser. Metallii No. 2 123 (1974).
30. O.A. Troitskii, Stal. No. 5 450 (1974).
31. K.M. Klimov, G.D. Shnyrev and I.I. Novikov, Dokl. Akad. Nauk. SSSR 219 323 (1974).
32. V.I. Spitsyn, O.A. Troitskii, V.G. Ryshkov and A.S. Kozyrev, Dokl. Akad, Nauk. SSSR 231 402 (1976).
33. V.I. Spitsyn, A.V. Kop'ev, V.G. Ryzhkov, N.V. Sokolov and O.A. Troitskii, Dokl. Akad. Nauk. SSSR 236 861 (1977).
34. O.A. Troitskii, V.I. Spitsyn, N.V. Sokolov and V.G. Ryzhkov, Dokl. Akad. Nauk. SSSR 237 1082 (1977).

35. O.A. Troitskii, V.I. Spitsyn and V.G. Ryzhkov, Dokl. Akad. Nauk. SSSR 243 330 (1978).
36. K.M. Klimov and I.I. Novikov, Russian Met. No. 6 127 (1978).
37. O.A. Troitskii, V.I. Spitsyn, N.V. Sokolov and V.G. Ryzhkov, Phs. Stat. Sol. (a) 52 85 (1978).
38. K.M. Klimov, A.M. Morukhovich, A.M. Glezer and B.V. Molotilov, Russian Met. No. 6 68 (1981).
39. A. San Martin, D.M. Nghiep, P. Paufler, K. Kleinstruck, U. Kramer and N.H. Guyen, Scripta Met. 14 1041 (1980).
40. V.L.A. Silveira, M.F.S. Porto and W.A. Mannheimer, Scripta Met. 15 945 (1981).
41. V.L.A. Silveira, R.A.F.O. Fortes and W.A. Mannheimer, Proc. 7th Interamerican Conf. Mat. Tech., Mexicon (October 1981) p. 722.
42. V.L.A. Silveira, R.A.F.O. Fortes and W.A. Mannheimer, Beitr. Electronemikorskop. Direktabb. Oberfl. 15 217 (1982).
43. S.T. Kishkin and A.A. Klypin, Dokl. Akad. Nauk. SSSR 211 325 (1973).
44. V. Ya. Kravchenko, J. Exptl. Theoret. Phys. (USSR) 51 1676 (1966).
45. K.M. Klimov, G.O. Shnyrev and I.I. Movikov, Sov. Phys. Dokl. 19 787 (1975).
46. A.M. Roshchupkin, V.E. Miloshenko and V.E. Kalinin, Sov. Phys. Solid State 21 532 (1979).
47. K. Okazaki, M. Kagawa and H. Conrad, Scripta Met. 12 1063 (1978).
48. K. Okazaki, M. Kagawa and H. Conrad, Scripta Met. 13 277 (1979).
49. K. Okazaki, M. Kagawa and H. Conrad, Scripta Met. 12 473 (1979).
50. K. Okazaki, M. Kagawa and H. Conrad, Mat. Sci. Engrg. 45 109 (1980).
51. K. Okazaki, M. Kagawa and H. Conrad, Titanium '80 Science and Technology, TMS-AIME (1980) p. 763.
52. S.K. Varma and L.R. Cornwell, Scripta Met. 14 1035 (1980).
53. P.D. Goldman, L.R. Motowidlo and G.M. Galligan, Scripta Met. 15 353 (1981).
54. A.A. Klypin, Metalloved. Term. Obrab. Met. No. 8 28 (1973).
55. A.A. Klypin, Problemy Prochnosti No. 7 20 (1975).
56. S.T. Kiskin and A.A. Klypin, Sov. Phys. Dokl. 18 502 (1974).
57. G.A. Verob'ev, S.G. Ekhanin, M.M. Milyushina and N.S. Nesmelov, Sov. Phys. Solid State 15 1695 (1974).
58. A.V. Zaretskii, Yu. A. Osip'yan and F.F. Petrenko, Sov. Phys. Solid State 20 829 (1978).
59. T. Okabe and A.G. Guy, Met. Trans. 1 2705 (1970).
60. F.A. Schmidt and O.N. Carlson, J. Less Common Met. 26 247 (1972).
61. F.A. Schmidt and O.N. Carlson, Met. Trans. 7A 127 (1976).
62. O.N. Carlson and F.A. Schidt, J. Less Common Met. 53 73 (1977).
63. F.M. d'Heurle, Met. Trans. 2 683 (1971).
64. F.M. d'Heurle, Physics of Thin Films, Vol. 7, G. Haas, M. Francombe and R. Hoffman, eds., Academic Press, NY (1973) p. 257.
65. F.M. d'Heurle and P.S. Ho, Thin Films - Interdiffusion and Reactions, J.M. Poate, K.N. Tu and J.W. Mayer, eds., Wiley-Interscience (1978) p. 243.
66. R.E. Hummel and H.B. Huntington, Electro- and Thermo-Transport in Metals and Alloys, TMS/AIME (1977).
67. B. Mishra and J.M. Siverston, Met. Trans. 14A 2255 (1983).
68. R.H. ZZee, G.J.C. Carpenter and F.A. Schmidt, Scripta Met. 18 489 (1984).
69. A.A. Klypin and E.S. Soloviev, Tsvet. Metallurgiya Izv. Vyashikh Ucheb. Zaved. No. 4 104 (1978).
70. A.A. Klypin, Termich. Obrabotka Metallov. No. 3 12 (1979).

71. T.J. Koppenaal and C.R. Simcoe, Trans. TMS/AIME 227 615 (1963).
72. Y. Onodera and K. Hirano, J. Mat. Sci. 11 809 (1976).
73. V.L.A. da Silveira, R.A.F. de Oliveira Fortes, 5th Congresso Brasileiro de Engenharia e Ciencia dos Materials (1982) p. 413.
74. V.L.A. da Silveira, J.L.B. Ribeiro, G.F.W. Soures and W.A. Mannheimer, Scripta Met. 18 131 (1984).
75. A.F. Sprecher, S.L. Mannan and H. Conrad, Scripta Met. 17 769 (1983).
76. H. Conrad, A.F. Sprecher and S.L. Mannan, "The Electroplastic Effect in Metals," Proc. Int. Symp. The Mechanics of Dislocations, Ed. by E.C. Alfantis and J.P. Hirth, MSM (1985) p. 225.
77. A.F. Sprecher, S.L. Mannan and H. Conrad, "On the Mechanisms for the Electroplastic Effect in Metals," to be published Acta Met.
78. H. Conrad, High Strength Materials, V.F. Zackay, ed., Wiley, NY (1965) p. 436.
79. A. Hikata, R.A. Johnson and L. Elbaum, Phys. Rev. Letters, 24 215 (1970).
80. T. Vreeland, Scripta Met. 18 645 (1984).
81. J.A. Gorman, D.S. Wood and T. Vreeland, J. Appl. Phys. 40 833, 903 (1969).
82. V.R. Parameswaran, N. Urabe and J. Weetman, J. Appl. Phys. 43 2982 (1972).
83. W.G. Ferguson, A. Kumar and J.E. Dorn, J. Appl. Phys. 38 1863 (1967).
84. W.P. Mason and A. Rosenberg, Phys. Rev. 151 434 (1964).
85. T.S. Hutchinson and D.H. Rogers, J. Appl. Phys. 33 792 (1962).
86. K. Marukawa, J. Phys. Soc. Jap. 11 499 (1967).
87. T. Suzuki, Dislocation Dynamics, A.R. Rosenfield, G.T. Hahn, A.L. Bement and R.I. Jaffee, eds. (1968) p. 551.
88. K.M. Jassby and T. Vreeland, Phys. Rev. 8 3537 (1973).
89. T. Suzuki, A.I. Kushime and M. Aoki, Acta Met. 12 1231 (1964).
90. G.A. Alers and D.O. Thompson, J. Appl. Phys. 32 283 (1961).
91. T. Vreeland, Dislocation Dynamics, A.R. Rosenfield, G.T. Hahn, A.L. Bement and R.I. Jaffee, eds. (1968) p. 529.
92. H. Conrad, N. Karam and S. Mannan, Scripta Met. 17 411 (1983).
93. H. Conrad, N. Karam and S. Mannan, Scripta Met. 18 275 (1983).
94. H. Hu and R.S. Cline, Trans. TMS-AIME 242 1013 (1968).
95. K. Okazaki and H. Conrad, Met. Trans. 3 2411 (1972).
96. P. Cottrill and P.R. Mould, Recrystallization and Grain Growth in Metals, Wiley, NY (1976).
97. Recrystallization of Metallic Materials, edited by F. Haessner, Dr. Ricderer - Verlag GmbH, Stuttgart (1978).
98. F.V. Lenel, Trans. AIME 203 158 (1955).
99. H. Conrad, P. Mazumdar, S. Wrinn and K. Bae, "Effect of a Coal Liquefaction Solvent on the Fatigue of 316 Stainless Steel at 300K: I. Behavior and Mechanisms in the Low-Cycle Regime," to be published Mat. Sci. Engr.
100. H. Conrad, Renewal Proposal to Army Research Office, "A Study into the Mechanism(s) for the Electroplastic Effect in Metals and Its Application to Metalworking, Processing and Fatigue," March 15, 1985.
101. J.A. Shepic and F.R. Schwartzberg, "Fatigue Testing of Stainless Steel," Rept. No. MCR-77-562, Martin Marietta Corp. (1977).
102. V.L.A. Silveira, R. Fortes and W. Mannheimer, Scripta Met. 17 1381 (1983).
103. F. Erdmann-Jesnit Zer, D. Mronka and K. Ouvier, Arch. Eisenhuttenw. 30 31 (1959).

104. F. Erdmann and K. Ouvier, Freiberger Forschungsh. 50B 136 (1960).
105. H. Kojima and T. Suzuki, Phys. Rev. Let. 21 896 (1968).
106. G. Kostorz, Phil. Mag. 27 633 (1973).
107. G. Kortorz, Acta Met. 21 813 (1973).
108. F. Iida, T. Suzuki, E. Kuramoto and S. Takeuchi, Acta Met. 27 637 (1979).
109. V.I. Startsev, V.V. Pustavalov, V.P. Soldtov, U.S. Femenko and T.I. Vainbald, Proc. 2nd Int. Conf. Metals and Alloys, Vol. 1, ASM, Cleveland (1970) p. 219.
110. G.A. Alers, O. Buck and B.R. Tittman, Phys. Rev. Letters; Proc. 2nd Int. Conf. Metals and Alloys, Vol. I, ASM, Cleveland (1970) p. 368.
111. A.V. Granato, Phys. Rev. Letters 27 660 (1971).
112. G. Kostorz, Phys. Stat. Sol. (5) 58 9 (1973).
113. T. Moriya and T. Suzuki, Internal Friction and Ultrasonic Attenuation in Solids, Univ. Tokyo Press (1977) p. 543.
114. L.P. Kubin and B. Jouffrey, Phil. Mag. 27 1369 (1973).
115. M.G. Ulitchny, A.K. Vasudevan and R. Gibala, Proc. 3rd Int. Conf. Strength of Metals and Alloys, Vol. I, ASM, Cleveland (1973) p. 505.
116. J.W. Christian, Met. Trans. 14A 1237 (1983).
117. F. Ackermann, H. Mugharabi and A. Seeger, Acta Met. 31 1353 (1983).
118. H. Conrad, Met. Sci. Engr. 6 265 (1970).
119. H. Conrad and H. Wiedersich, Acta Met. 8 128 (1960).
120. G. Schoeck, Phys. Stat. Sol. 8 499 (1965).
121. U.F. Kocks, A.S. Argon and M.F. Ashby, Prog. Mat. Sci. 19 1 (1975).
122. H. Conrad, NPL Symp. No. 15 The Relation Between the Structure and Mechanical Properties of Metals, Vol. 2 HMSO (1963) p. 475.
123. J.E. Dorn and S. Rajnak, Trans. TMS-AIME 230 1052 (1964).
124. Y.T. Chen, D. Atteridge and W. Gerberich, Acta Met. 29 1171 (1981).
125. A. Seeger, Z. Metal. 72 369 (1981).
126. G.H. Stone and H. Conrad, Acta Met. 12 1125 (1964).
127. H. Conrad and G. Stone, High Temperature Refactory Metals, Part 2, Gordon and Breech (1966) p. 215.
128. J. Fries, B. Houssin, G. Cizeron and P. Lacombe, J. Less-Common Met. 33 117 (1973).
129. F. Guiu and M. Anglada, Phil. Mag. A. 46 881 (1982).
130. A. Seeger and Ch. Wuthrich, Nuova Cin. 33B 38 (1976).
131. F. deLima and W. Benoit, Phys. Stat. Sol. (a) 67 565 (1981).
132. H. Conrad and T. Tanaka, unpublished work, University of Kentucky (1973).
133. H.D. Guberman, Acta Met. 16 713 (1968).
134. M.S. Duesbery, Acta. Met. 31 1759 (1983).

Table 1. Characteristics of the electroplastic effect in metals identified by Troitskii and co-workers. Current density $J \simeq 10^3$ A/mm^2, pulse duration $t_D \simeq 50$ μs, pulse frequency $f_p = 0.1$ Hz; temperature of test T = 78-300K. ΔP = load drop associated with current pulse, P = total load.

I. Characteristics of the electroplastic effect in Zn crystals

- ΔP varies with crystal orientation, being a maximum at $X_o \approx 45°$-60°.
- ΔP increases significantly with addition of 0.02% Cd.
- ΔP increases approximately linearily with J.
- ΔP increases with decrease in temperature.
- ΔP tends to decrease with increase in strain rate, but effect is not straightforward.
- ΔP increases with change in current direction--i.e., there exists a polarity effect.
- $\Delta P/P$ = 10-40%.
- ΔP occurs in compression as well as tension.

II. Other Observations

- Similar effects occurred in Cd, Zn, Pb and In single crystals.
- Electroplastic effect also occurred in polycrystals--same magnitude of ΔP, but smaller $\Delta P/P$ (1-8%).

III. Explanation

Electroplastic effect is mainly due to the interaction of drift electrons with dislocations:

- Additional force on dislocations due to an electron wind.
- Effect on dislocation vibrational frequency.
- Effect on obstacle strength opposing motion of dislocation.

Table 2. Effects of current pulses on metalworking (Cu, Fe, stainless steel, W).

- Reduction in force required for working.
- Reduction in brittleness.
  - Can roll W sheet at room temperature.
- Imorovement in surface finish.
- Improvement in subsequent mechanical properties of product.
  - Increase in tensile strength and elongation.
- Changes in texture.
- Changes in microstructure.

Table 3. Theoretical estimates of the coefficients K_{ew} and B_{ew} due to an electron wind acting on dislocations.

	K_{ew} (10^{-9} $\frac{dyne}{cm}$/A/cm^2)			B_{ew} (10^{-5} dyne-s/cm^2)		
Metal	Eq. 1	Eq. 2	Eq. 3	Eq. 1	Eq. 2	Eq. 3
Al	0.13	7.71	26.4	0.13	7.71	26.3
Cu	0.09	7.58	26.4	0.12	10.10	35.0
Ni	0.08	7.77	26.4	0.12	12.0	40.5
Fe	0.12	6.54	26.4	0.11	6.10	24.5
Nb	0.30	5.89	26.4	0.13	2.63	11.7
W	0.53	4.58	26.4	0.13	1.10	6.3
Ti	0.22	3.14	26.4	0.14	0.19	1.6

NOTES:

Kravchenko (44): $f/\ell = [\frac{b}{4}(\frac{3n}{2E_F})\frac{\Delta^2}{v_F}](v_e - v_d) = (\frac{3b}{8}\frac{\Delta^2}{eE_F v_F})J$ (1)

Klimov et al. (45): $f/\ell = \frac{1}{3} n m^* b v_F (v_e - v_d) = \frac{m^* b v_F}{3e} J$ (2)

Roschupkin et al. (46): $f/\ell = \frac{2h}{\pi} n(v_e - v_d) = \frac{2h}{\pi e} J$ (3)

$K_{ew} = (f/\ell)/J$ (Electron wind force factor)

$B_{ew} = (f/\ell)/v_e = [\frac{(f/\ell)}{J}]en = \kappa_{ew}\, en$ (Electron wind push coefficient)

v_e = electron velocity = J/en

e = electron charge = 1.602 X 10^{-19} Coulombs

J = current density (1 Amp/cm^2 = 6.25 x 10^{18} e/cm^2 -s)

n = electron density = number per unit volume

E_F = Fermy energy; v_F = Fermi velocity

m^* = effective electron mass

v_d = dislocation velocity ≈ 0 (Assume dislocation is temporarily held up at obstacle.)

h = Planck's constant = 6.62 x 10^{-27} erg-s

Table 4. Publications and Patents Pertaining to Work on the ARO Research Contract

A. Publications

I. Mechanisms for the Electroplastic Effect

1. A.F. Sprecher, S.L. Mannan and H. Conrad, "On the Temperature Rise Associated with the Electroplastic Effect in Titanium," Scripta Met. 17 769 (1983).

2. H. Conrad, A.F. Sprecher and S.L. Mannan, "The Elastroplastic Effect in Metals," The Mechanics of Dislocations, ed. by E.C. Alfantis and J.P. Hirth, ASM (1985) p. 225.

3. A.F. Sprecher, S.L. Mannan and H. Conrad, "On the Mechanisms for the Electroplastic Effect in Metals," to be published Acta Met.

4. H. Conrad, Reply to Discussion by J.I. Dickson, L. Handfield and G.L. Esperance to above paper, Metall. Trans. 16A 695 (1985).

5. H. Conrad, "Plastic Flow and Fracture of Titanium at Low Temperatures," Cryogenics 24 293 (1984).

II. Effects of Repeated Current Pulses on the Recovery, Recrystallization and Grain Growth of Metals.

1. H. Conrad, N. Karam and S.L. Mannan, "Effect of Electric Current Pulses on the Recrystallization of Copper," Scripta Met. 17 411 (1983).

2. H. Conrad, N. Karam and S.L. Mannan, "Effect of Prior Cold Work on the Influence of Electric Current Pulses on the Recrystallization of Copper," Scripta Met. 18 275 (1984).

3. H. Conrad, M. Swintowski and S.L. Mannan, "Effect of Cold Work on Recrystallization Behavior and Grain Size Distribution in Titanium," Metall. Trans. 16A 703 (1965).

B. Patents

1. H. Conrad, Invention Disclosure No. 78B-D053-83, "Enhancement of Solid State Reactions and Transformations by the Application of Electric Current," submitted Jan. 18, 1983 to NCSU University Patent Committee.

Table 5. Theses Completed by Students Working on the Project

A. M.S. Theses

1. S.K. Mannan, "The Effect of Electric Current on Solid State Transformations in Titanium, Copper and High Carbon Steel," NCSU, September 5, 1985.

B. Ph.D. Theses

1. A.F. Sprecher, Jr. "The Electroplastic Effect in Metals," NCSU, December, 1984.

2. N.H. Karam, "Kinetics and Mechanisms of Low Temperature Deformation in High Purity Niobium Single Crystals," NCSU, May, 1985.

Table 6. Seeger's theory for the temperature and strain rate dependence of the flow stress of BCC metals based on kink formation and migration.

Relative Value of Effective Stress τ	Relative Temp.	Stress Dependence of Kink-Pair Formation Enthalpy	Analytical Approx.	$\dot{\gamma}_o$	$H_{kp}(\tau^*)$	v^*
Very Small ($x \ll 1$)	High	Elastic Interaction (E.I.) of Kinks	Diffusion (D_k) Approx.	$(2n)^{1/2}\rho_m Lab\left(\frac{2H_k D_k}{w_k^2 \gamma_o a^2}\right)\left(\frac{2\alpha}{kT}\right)^{3/2}(\tau^*)^{4/3}$	$2H_k - 2\alpha(\tau^*)^{1/2}$	$kT\left[\left(\frac{\partial \ell n \dot{\gamma}}{\partial \tau^*}\right)_T - \frac{3}{4\tau^*}\right]$
Small ($x \gg 1$)	Intermed.	Elastic Interaction (E.I.) of kinks	Transition-State (T.S.) Approx.	$2\pi\,\rho_m Lab(\pi\, m_k kT)^{-1/2}(H_k/w_k^2)$	$2H_k - 2\alpha(\tau^*)^{1/2}$	$kT\left\{\left(\frac{\partial \ell n \dot{\gamma}}{\partial \tau^*}\right)_T - \frac{1}{\cosh\phi}\left(\frac{\partial \ell n x}{\partial \tau^*}\right)_T\right\} = \alpha(\tau^*)^{-1/2}$
Large	Low	Line-Tension of Dislocation	Line-Tension (L.T.) Approx.	$2\pi\,\rho_m Lab(\pi\, m_k kT)^{-1/2}(H_k/w_k^2)$	$2H_k\left\{1 - \frac{\tau^*}{2\sqrt{3}\,\tau_p}\left[1 - \ell n\left(\frac{\tau^*}{12\sqrt{3}\,\tau_p}\right)\right]\right\}$	$kT\left\{\left(\frac{\partial \ell n \dot{\gamma}}{\partial \tau^*}\right)_T - \frac{1}{\cosh\phi}\left(\frac{\partial \ell n x}{\partial \tau^*}\right)_T\right\}$
Very Large ($\tau^* \to \tau_p$)	Very Low	Line-Tension of Dislocation	Line-Tension (L.T.) Approx.	$2\pi\,\rho_m Lab(\pi\, m_k kT)^{-1/2}(H_k/w_k^2)$	$1.48\,2H_k\left(\frac{\tau_p - \tau^*}{\tau_p}\right)^{5/2}$	$kT\left(\frac{\partial \ell n \dot{\gamma}}{\partial \tau^*}\right) = \frac{5H_{kp}}{2(\tau_p - \tau^*)}$

$\tau^* = \tau - \tau_\mu$ = effective stress

$\dot{\gamma}_o$ = pre-exponential factor

$H_{kp}(\tau^*)$ = enthalpy of a pair of kinks of opposite sign in its saddle point configuration ($\equiv \Delta G_{kp}$)

v^* = activation volume = $-(\partial H_{kp}/\partial \tau^*)_T$

$x = 2(2m_k)^{1/2}\lambda_1 \mu_k \equiv \sinh\phi$

m_k, w_k, μ_k = mass, width and mobility of kinks

$\lambda_1^2 = (2b\tau^*)^2 (a/\gamma_o)^{1/2}$

a = spacing between Peierls valleys

b = Burgers vector

ρ_m = density of screw dislocations

$2H_k$ = enthalpy of formation of a pair of isolated kinks

$D_k = \mu_k kT$ = kink diffusivity

$\gamma_o = Kb^2/4\pi$; $K = \{S_{11}/S_{44}(S_{11}S_{44} - S_{15}^2)\}^{1/2}$

$\alpha = (a^3 b \gamma_o/2)^{1/2}$

τ_p = Peierls-Nabarro stress at T = 0K

Table 7. Comparison of the values of $2H_k$ and $\dot{\gamma}_o$ obtained in the present tests on Nb with those obtained by others.

Authors	Ref.	Year	Property	Form	$2H_k$ (ev)	$\dot{\gamma}_o$ (s^{-1})
Conrad	122	1963	Yield and flow stresses from literature	polycrystalline	0.60	10^6-10^8(*)
Stone & Conrad	126	1964	Creep	polycrystalline	0.68	1.6×10^8 (*)
Conrad & Stone	127	1966	Yield and flow stresses	polycrystalline	0.68	2.2×10^8 (*)
Fries et al.	128	1973	Yield and flow stresses	polycrystalline	0.64	---
Kubin & Jouffrey	114	1973	Yield stress	single crystal	0.64	1×10^7
Guiu & Anglada	129	1982	Cyclic deformation	single crystal	0.65	2×10^8 (*)
Ackermann et al.	117	1983	Cyclic deformation	single crystal	0.65	1×10^7
Karam & Conrad	Present	1985	Yield and flow stresses	single crystal	0.66	1.5×10^7
Seeger & Wuthrich	130	1976	Internal friction	single crystal	0.65	
DeLima & Benoit	131	1981	Internal friction	single crystal	0.61	
Conrad & Tanaka	132	1973	Analysis of dislocation velocity data of Gubermann (133)	single crystal	0.65	
Seeger & Wuthrich	130	1976	Theoretical estimate of kink-pair formation in α-Fe		1.2	
Duesberry	134	1983	Theoretical estimate of kink-pair formation in α-Fe		0.74	

*Obtained from a plot of ΔH^* versus temperature and therefore the value reported is for the product $\dot{\gamma}_o \exp. \Delta S^*/k$.

List of Illustrations

300X, (c) no current, 1000X and (d) J = 0.1 A/mm^2, 1000X. Arrows show crack nucleation sites.

Fig. 17 Effect of 1.0 A/mm^2 continuous current on the S-N_f curve for 316 stainless steel tested in rotating bending at room temperature. Also included is the result for one test in which the specimen was heated 12°C by forced hot air and tested without current.

Fig. 18 Effect of continuous d.c. current of 10 A/mm^2 on the annealing behavior of Cu cold worked 22%.

Fig. 19 Effect of a continuous d.c. current of 31 A/mm^2 on the annealing behavior of Cu cold worked 76%.

Fig. 20 Effect of a continuous d.c. current of 6.5 A/mm^2 on the tempering (t = 1/2 hr) of a hardened AISI (02) tool steel.

Fig. 21 Effect of a continuous d.c. current of 6.5 A/mm^2 on the microstructure of a hardened AISI (02) tool steel tempered for the fixed time and temperature of 30 min at ~ 600K: (a) J = 6.5 A/mm^2, 611K and (b) no current, 591K.

Fig. 22 Effect of a continuous d.c. current of 6.5 A/mm^2 on the microstructure of a hardened AISI (02) tool steel tempered to a constant hardness of ~ 410 VHN: (a) 30 min at 787K with J = 6.5 A/mm^2 and (b) 30 min at 679K with no current.

Fig. 23 Effect of temperature on the yield stress (τ_f) and on the thermal and athermal components of the flow stress (τ^* and τ_μ) for Nb single crystals. Letter N at 4.2K indicates test was conducted in the "normal state" obtained by application of a magnetic field.

Fig. 24 Variation of the activation volume $v = kT\partial \ell n \dot{\gamma}/\partial \tau$ with temperature for Nb single crystals from strain rate cycling and stress relaxation tests.

Fig. 25 Variation of the activation enthalpy ΔH^* and the Gibbs free energy of activation ΔG with temperature for the plastic deformation of Nb single crystals at a tensile strain rate of 1.66 x 10^{-4} s^{-1}.

Fig. 26 The temperature dependence of τ^* showing the different approximations in Seeger's model (117, 125)

Fig. 27 The temperature dependence of the activation volume v showing the different approximations in Seeger's model (117,125).

Fig. 28 Values of $2H_k$ derived using the transition state approximation at various stress levels.

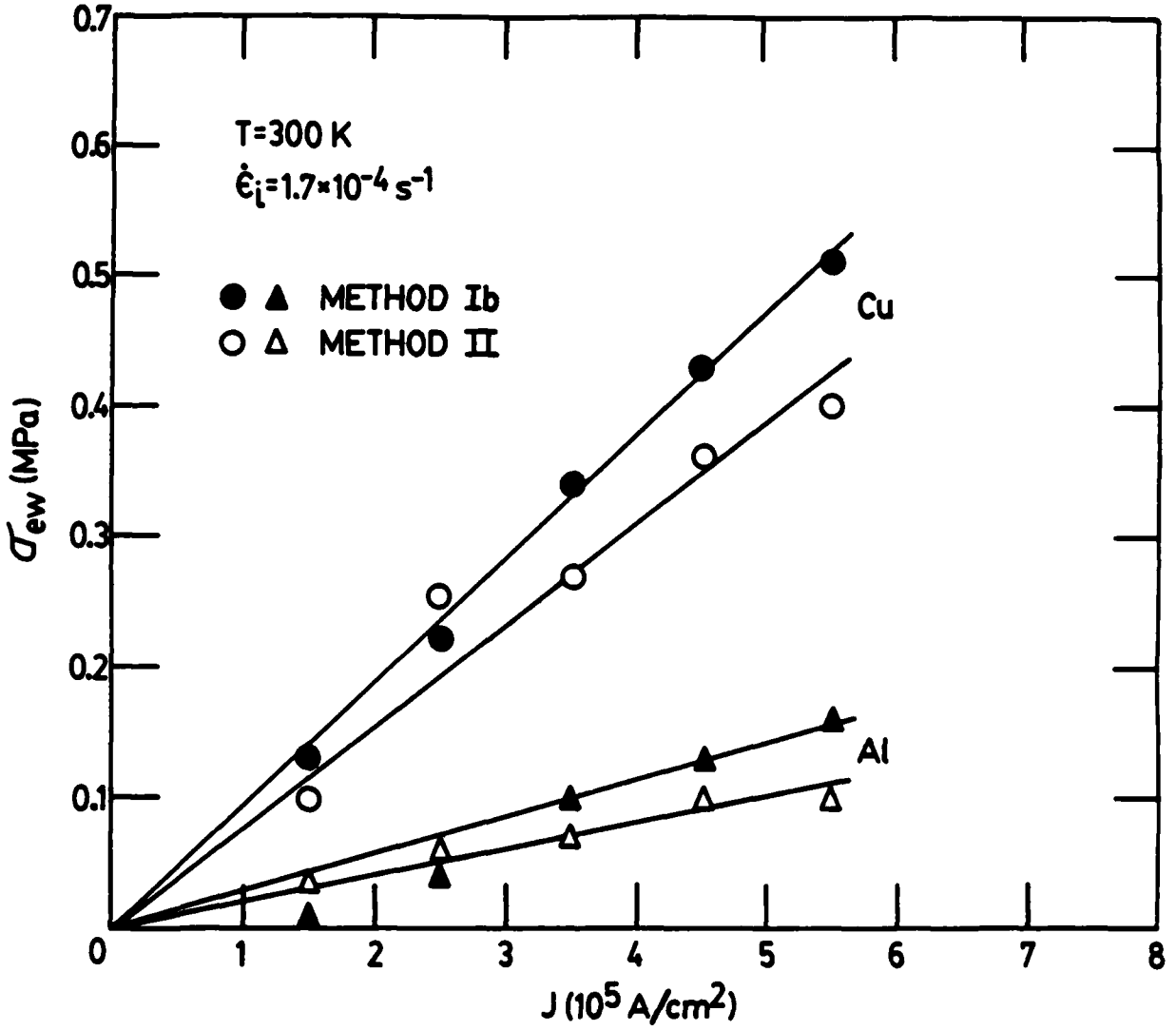

Fig. 2 σ_{ew} versus J for Al and Cu by two methods.

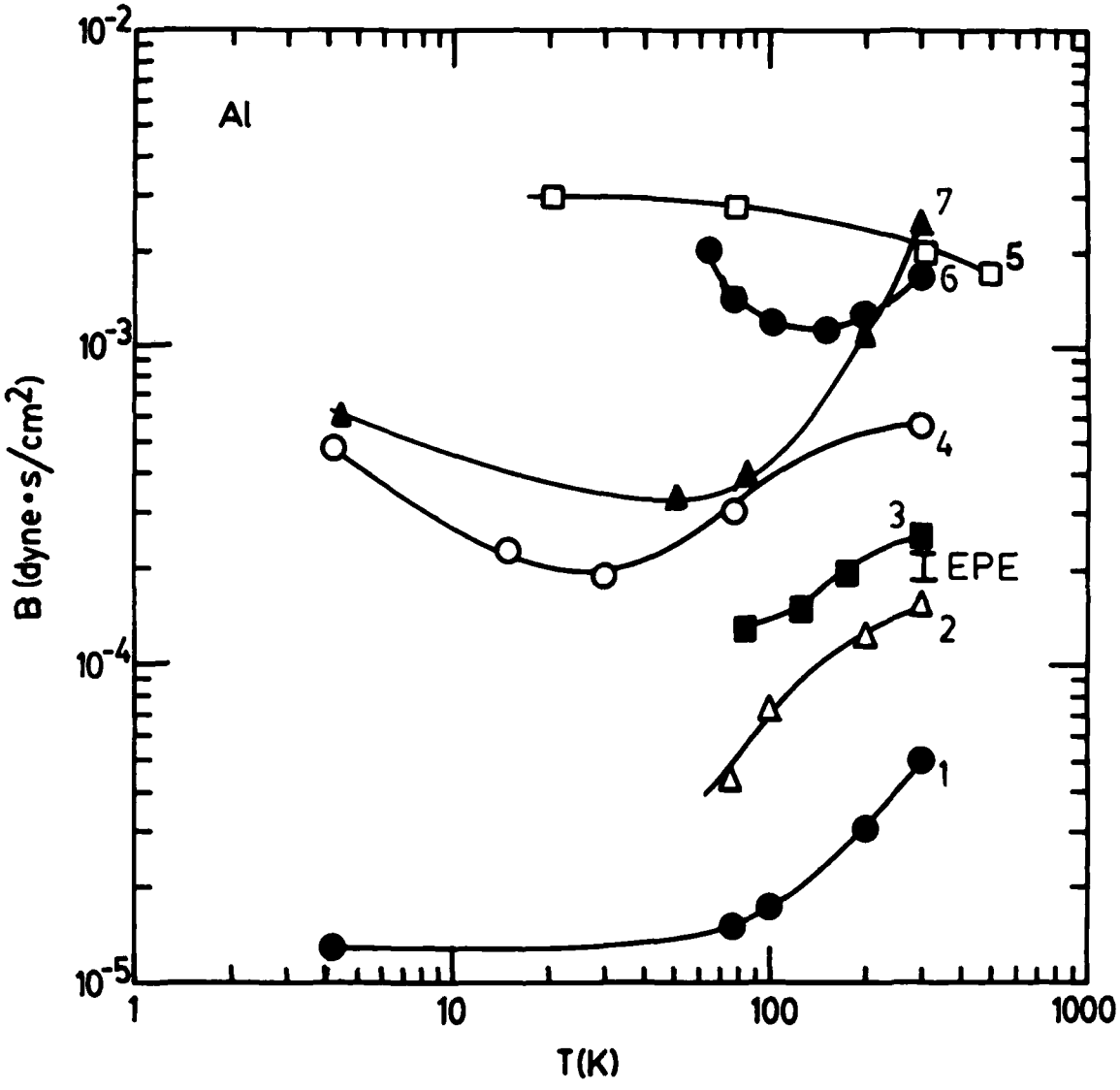

Fig. 3 Dislocation damping constant B for Al as a function of temperature. 1-(79); 2-(80); 3-(81); 4-(82); 5-(83); 6-(84); 7-(85). EPE represents present results based on electroplastic effect.

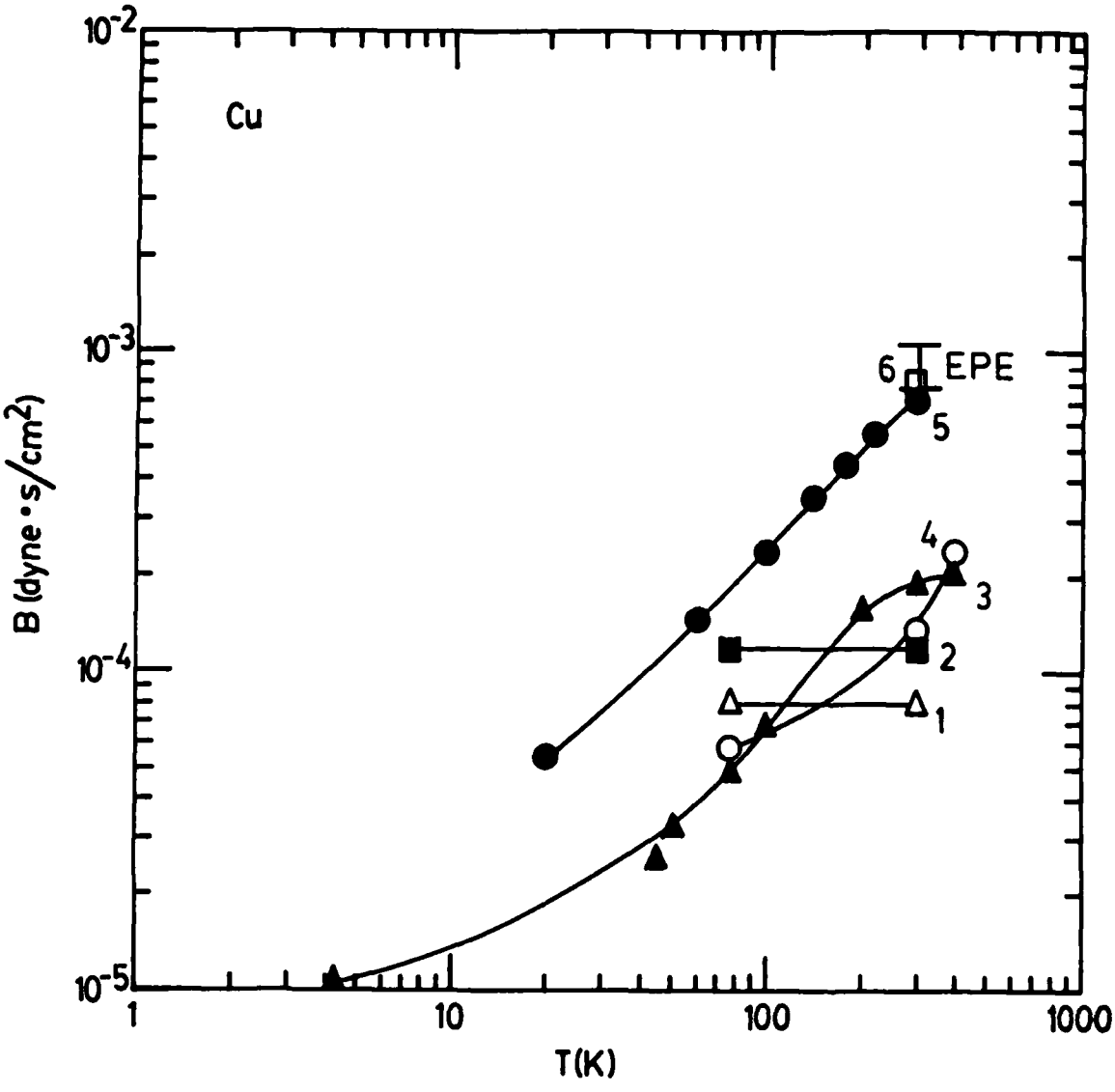

Fig. 4 Dislocation damping constant B for Cu as a function of temperature. 1-(86); 2-(87); 3-(88); 4-(89); 5-(90); 6-(91). EPE represents present results based on electroplastic effect.

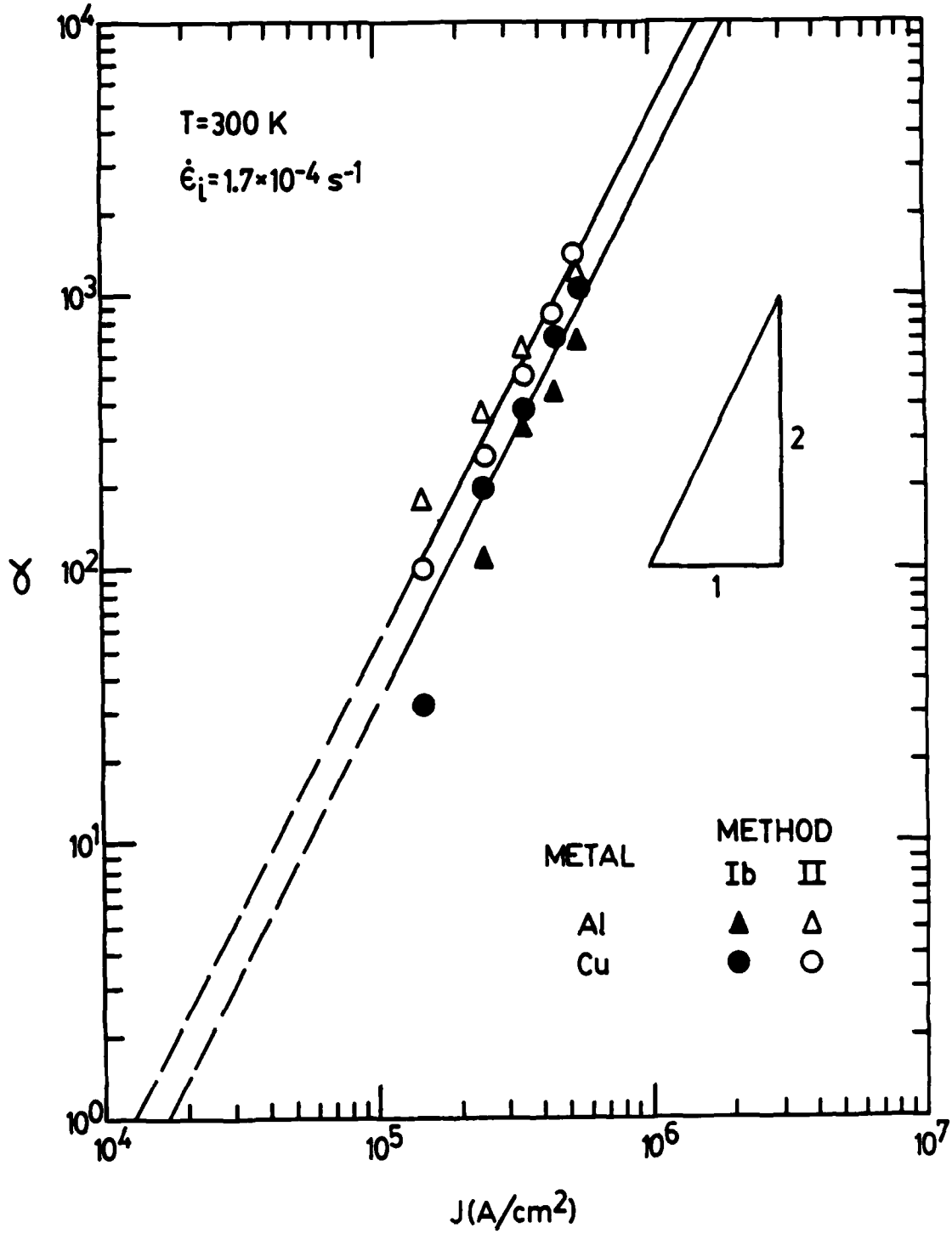

Fig. 5 Log-log plot of the parameter α versus J.

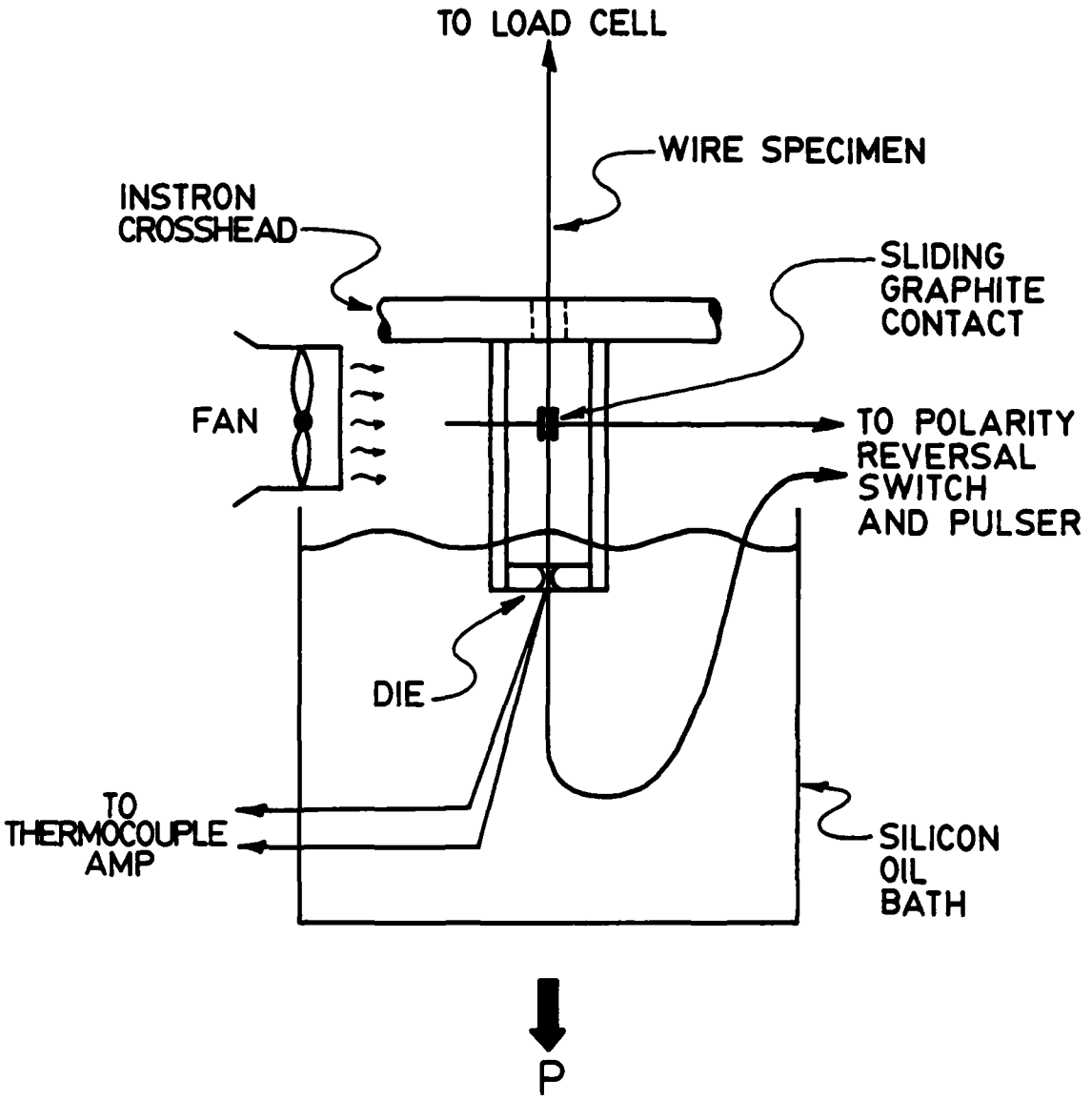

Fig. 6 Schematic of the set-up for wire drawing.

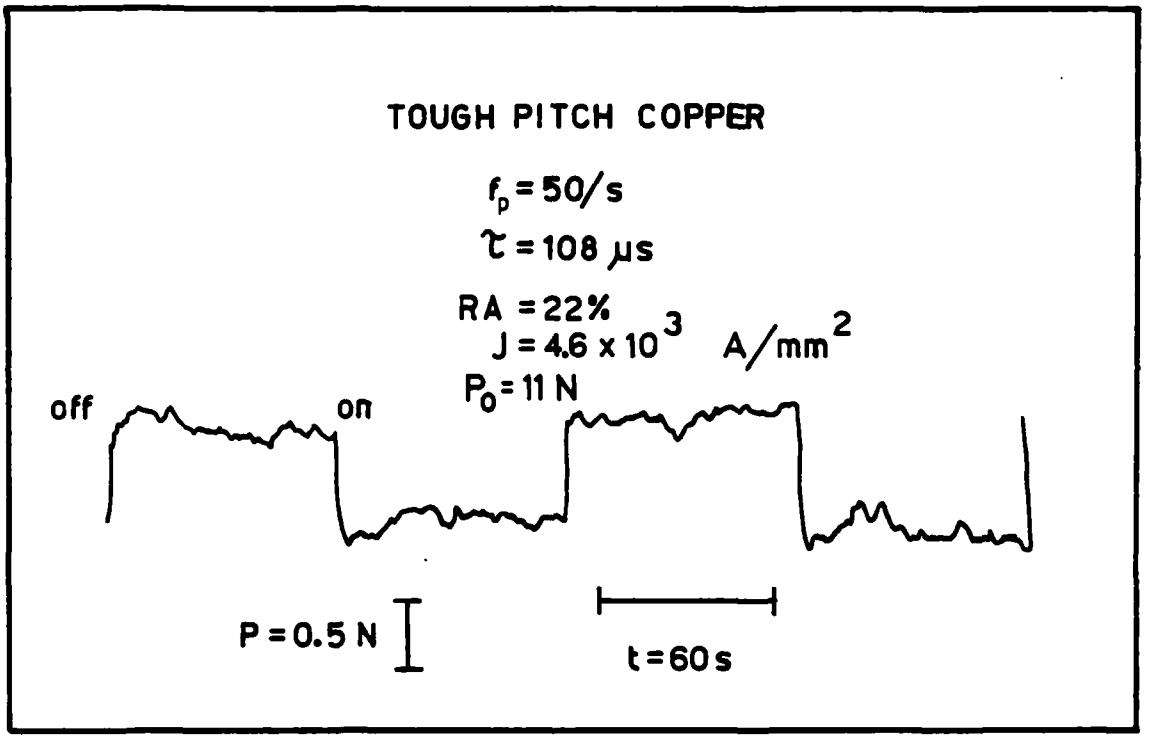

Fig. 7 Load versus time for the drawing of Cu wire without, and with, repeated current pulses.

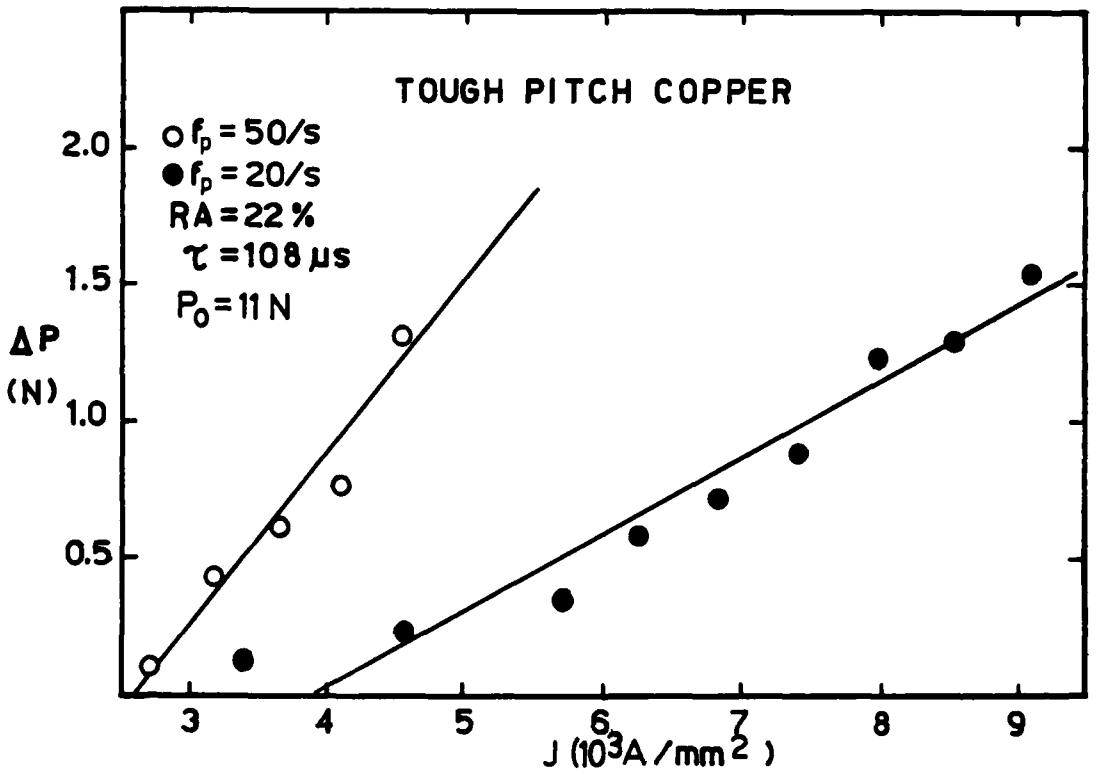

Fig. 8 Effect of current density on the drop in drawing force for Cu wire as a function of the frequency of the current pulses.

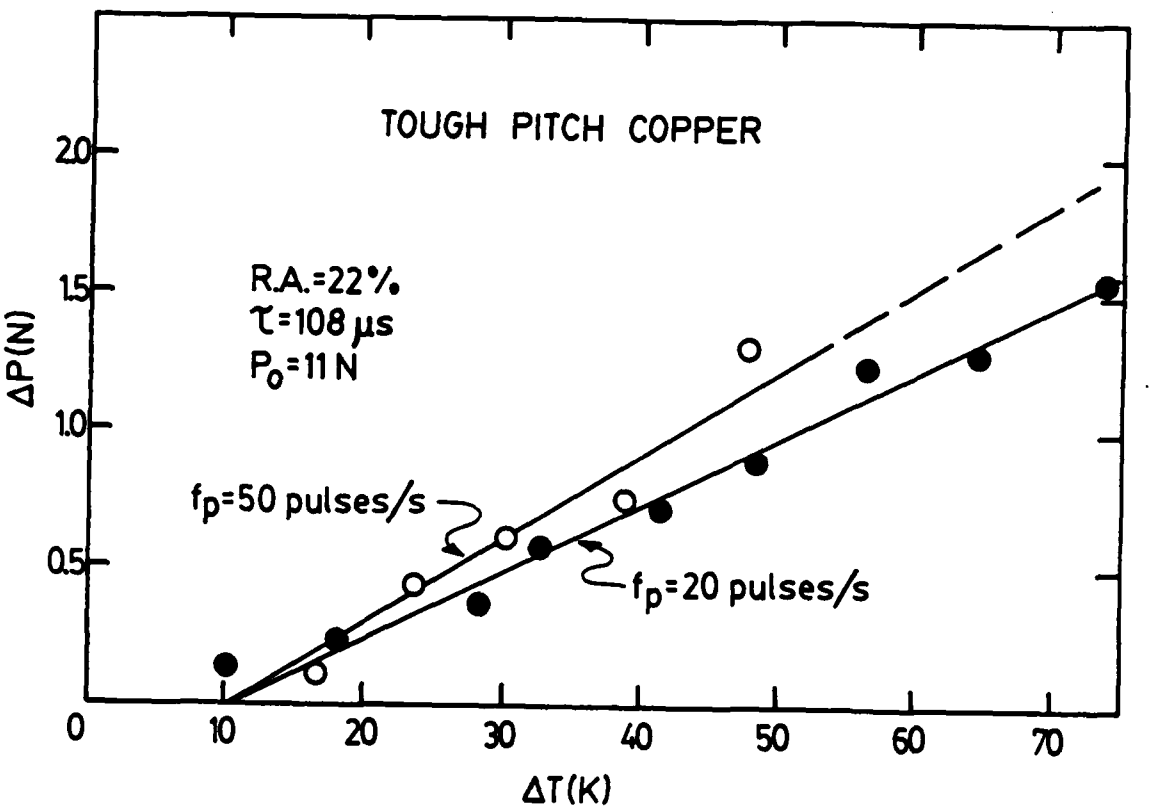

Fig. 9 ΔP versus the temperature rise ΔT as a function of pulse frequency for the drawing of Cu wire.

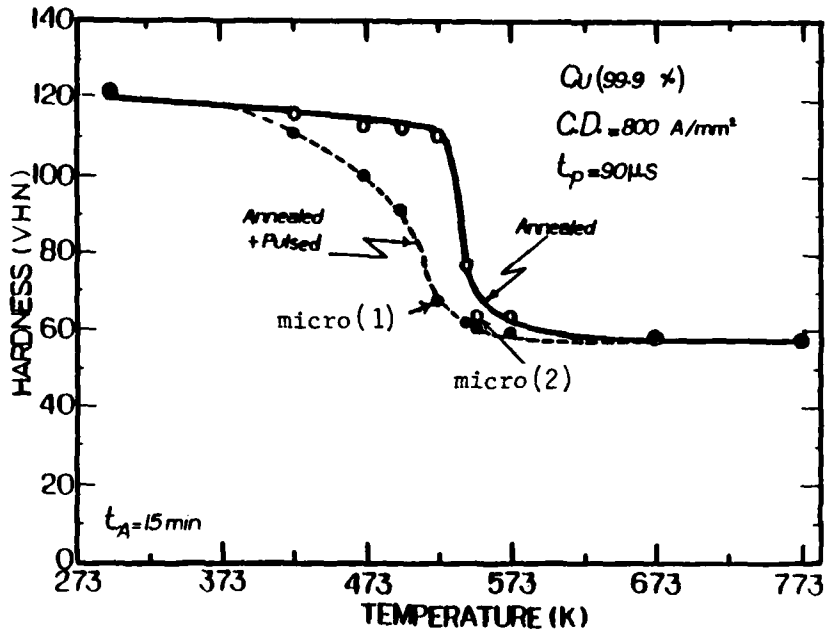

a. Hardness versus temperature for annealed-only and annealed-plus-pulsed specimens of Cu.

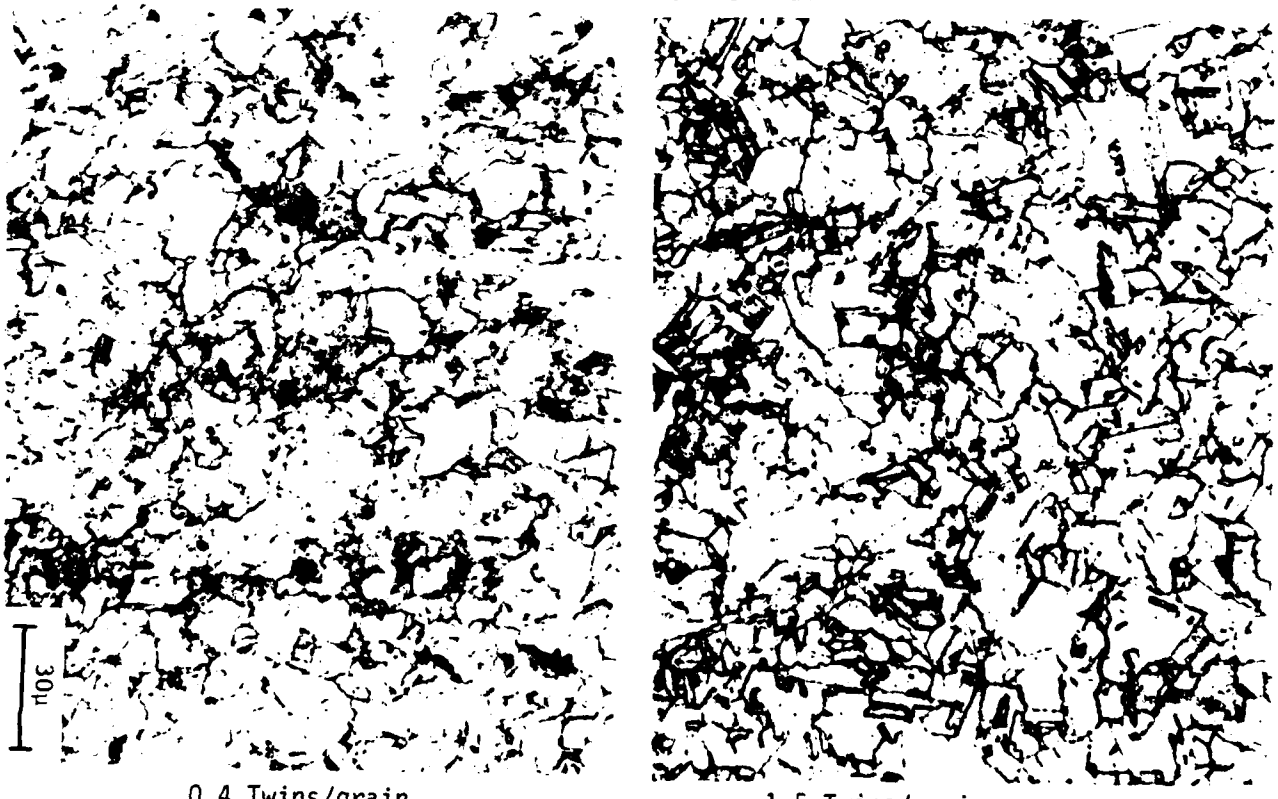

0.4 Twins/grain
(1) X600, 498°K Annealed + pulsed

1.5 Twins/grain
(2) X600, 548°K Annealed only

b. Microstructure at comparable degree of recrystallization (V.H.N.≅64)

Figure 10. Effect of electric current pulses on the recovery and recrystallization behavior of Cu. (a) Hardness versus temperature for annealed-only and annealed-plus-current pulsed specimens and (b) microstructure at a comparable degree of recrystallization.

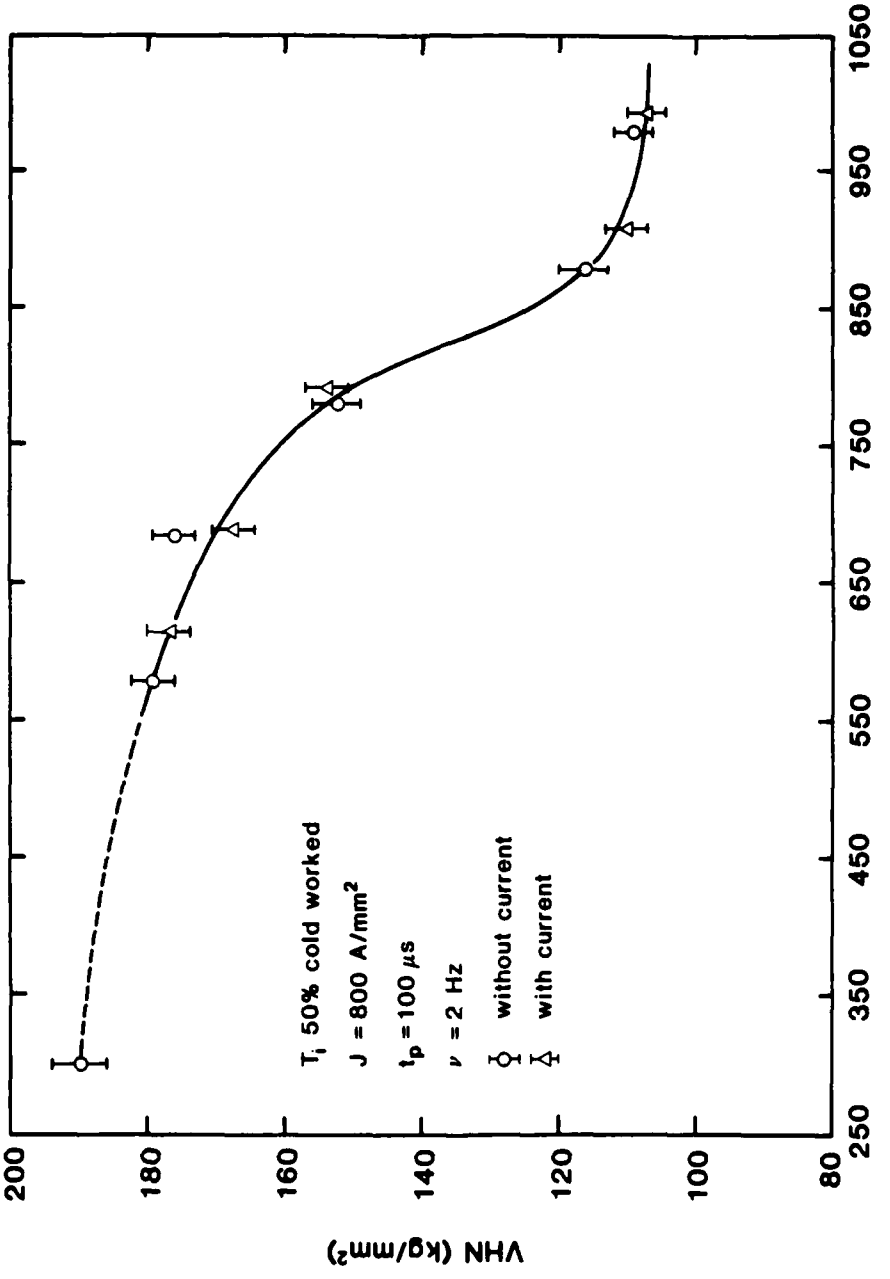

Fig. 11 Vickers hardness versus temperature for the annealing of Ti without, and with, current pulses.

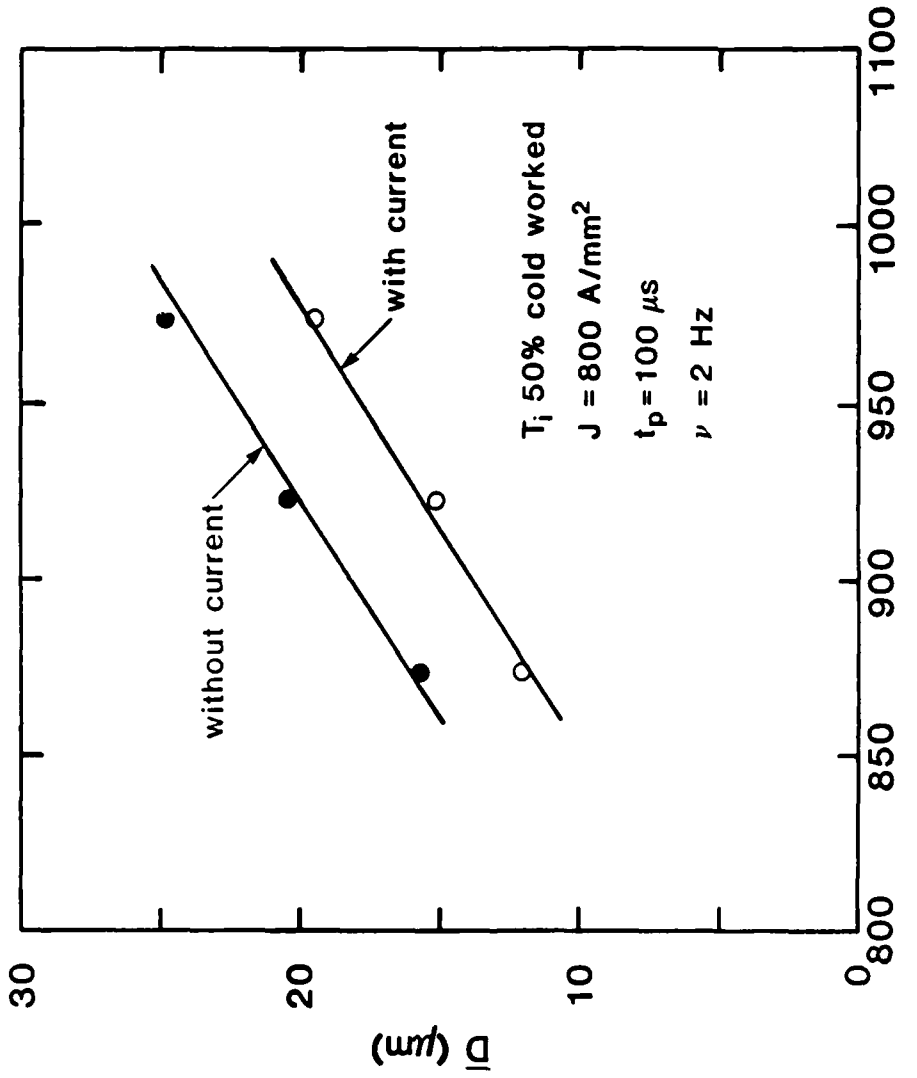

Fig. 12 Mean linear intercept grain size D versus temperature for the annealing of Ti without, and with, current pulses.

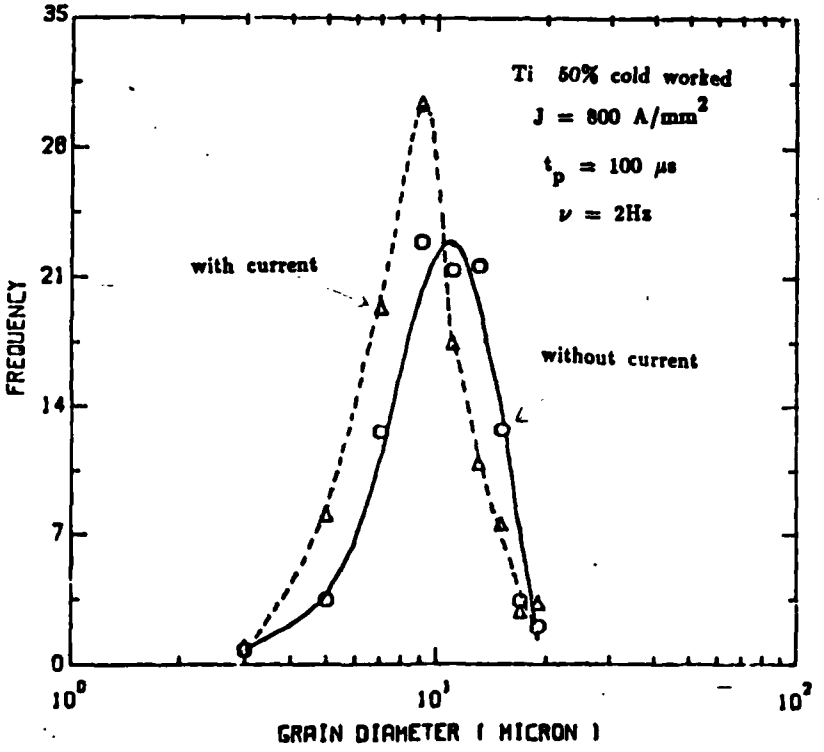

Fig. 13 Grain size distribution in Ti annealed at 873K without, and with, current pulses.

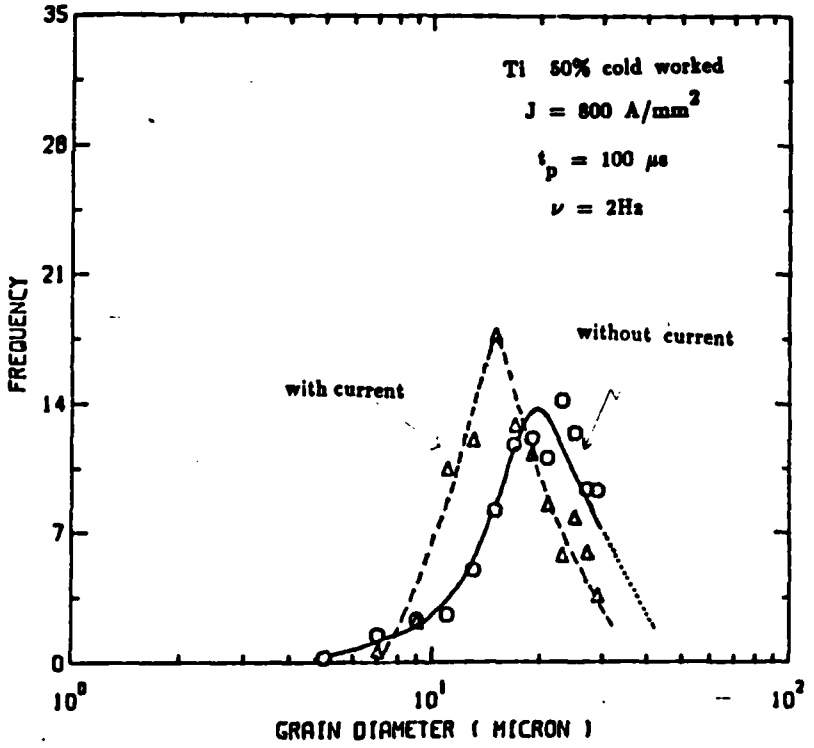

Fig. 14. Grain size distribution in Ti annealed at 973K without, and with, current pulses.

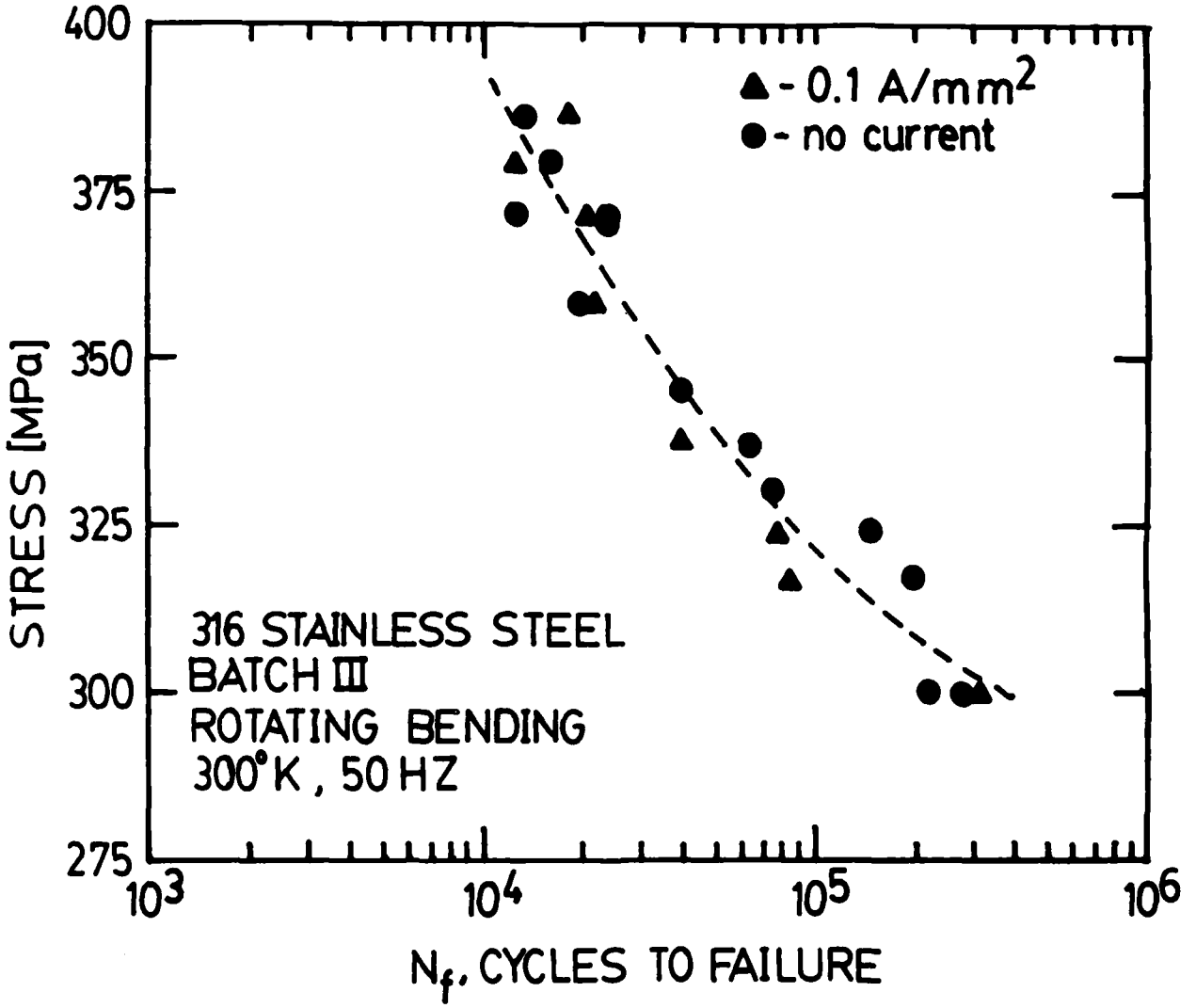

Fig. 15 Effect of 0.1 A/mm^2 continuous d.c. current on the S-N_f curve for 316 stainless steel tested in rotating bending at room temperature.

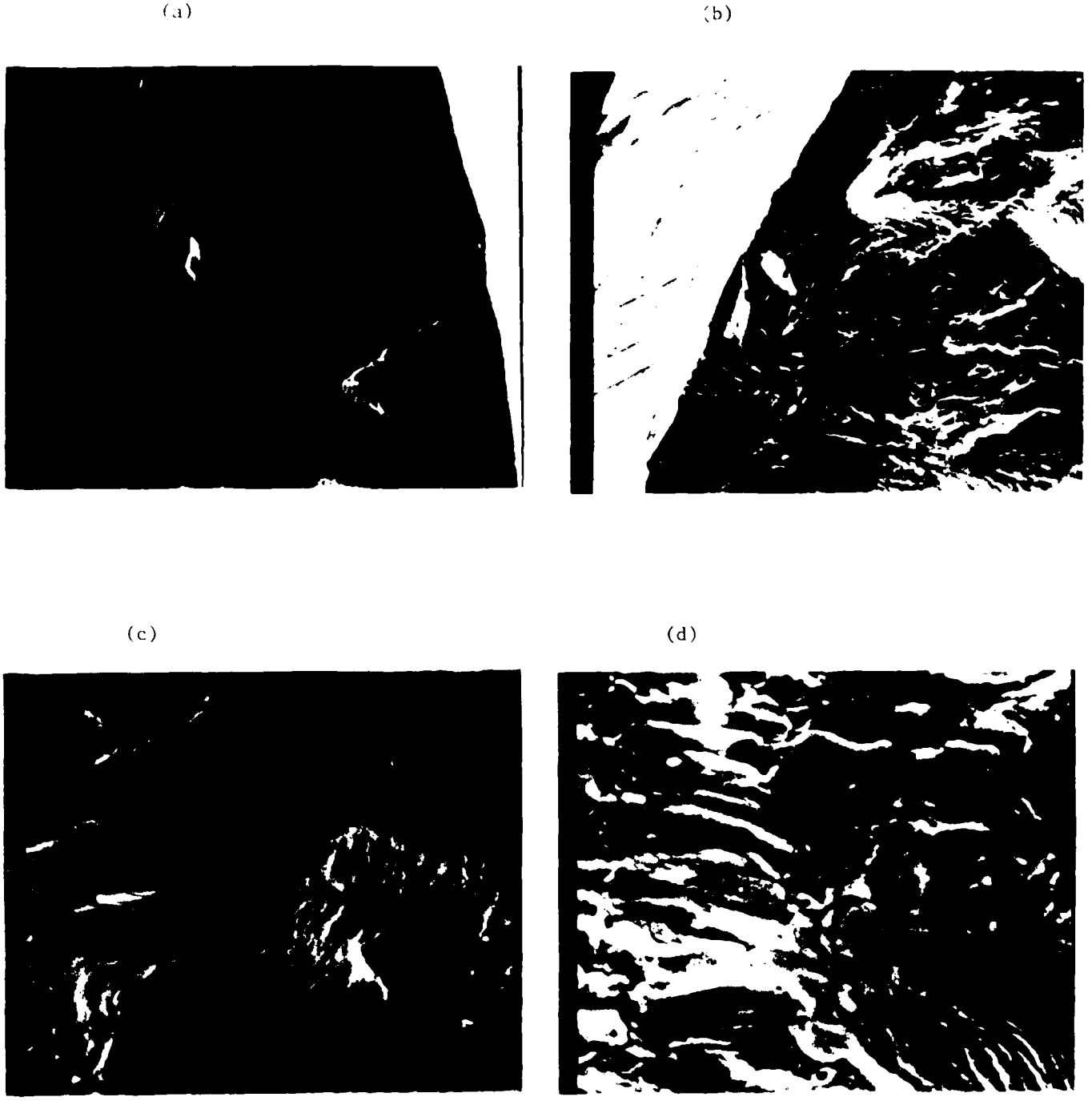

Fig. 16 SEM micrographs at two magnifications of the fracture surfaces of 316 stainless steel specimens tested in rotating bending fatigue with, and without, the concurrent application of continuous d.c. current: (a) no current, 300X, (b) J = 0.1 A/mm^2, 300X, (c) no current, 1000X and (d) J = 0.1 A/mm^2, 1000X. Arrows show crack nucleation sites.

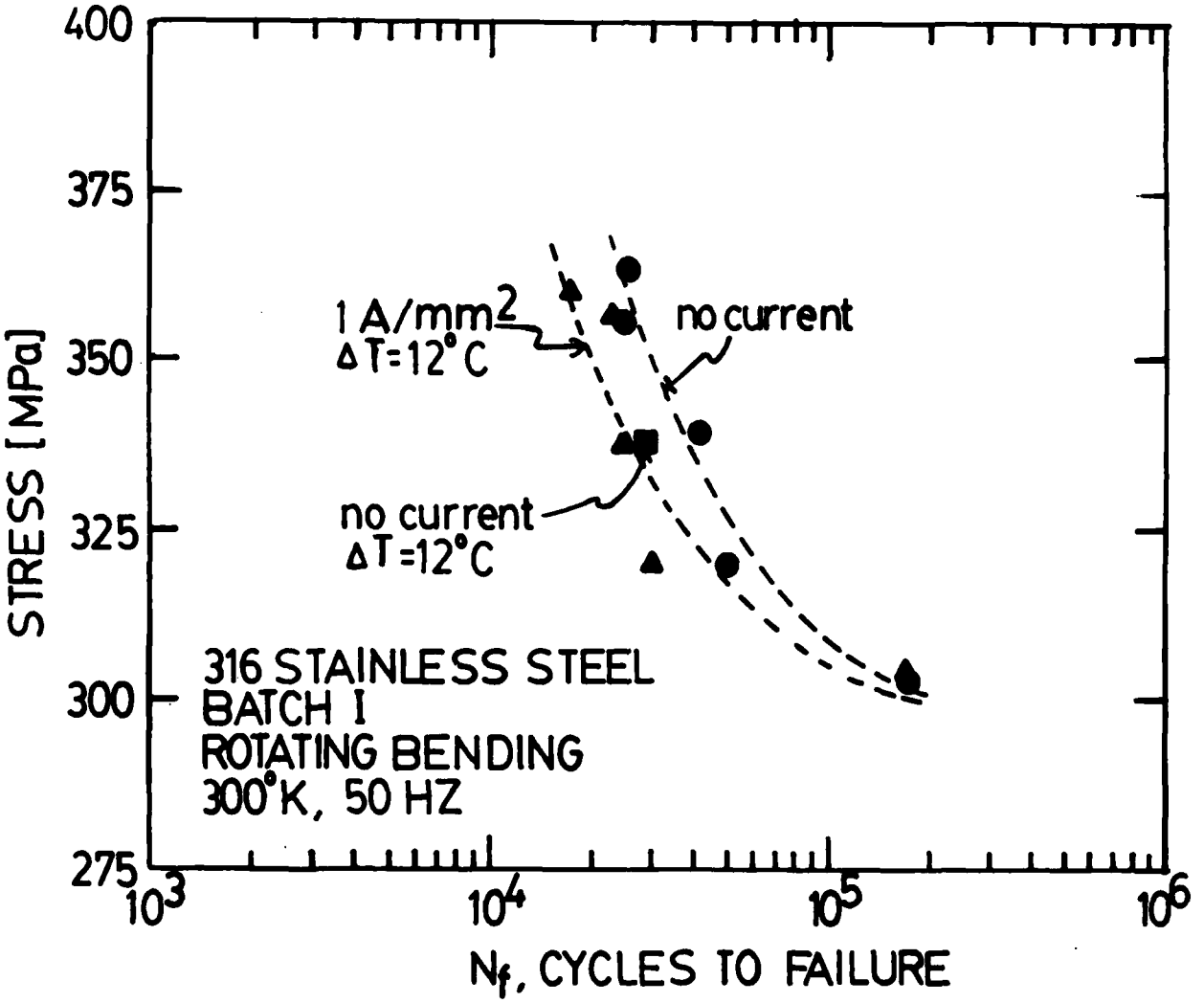

Fig. 17 Effect of 1.0 A/mm^2 continuous current on the S-N_f curve for 316 stainless steel tested in rotating bending at room temperature. Also included is the result for one test in which the specimen was heated 12°C by forced hot air and tested without current.

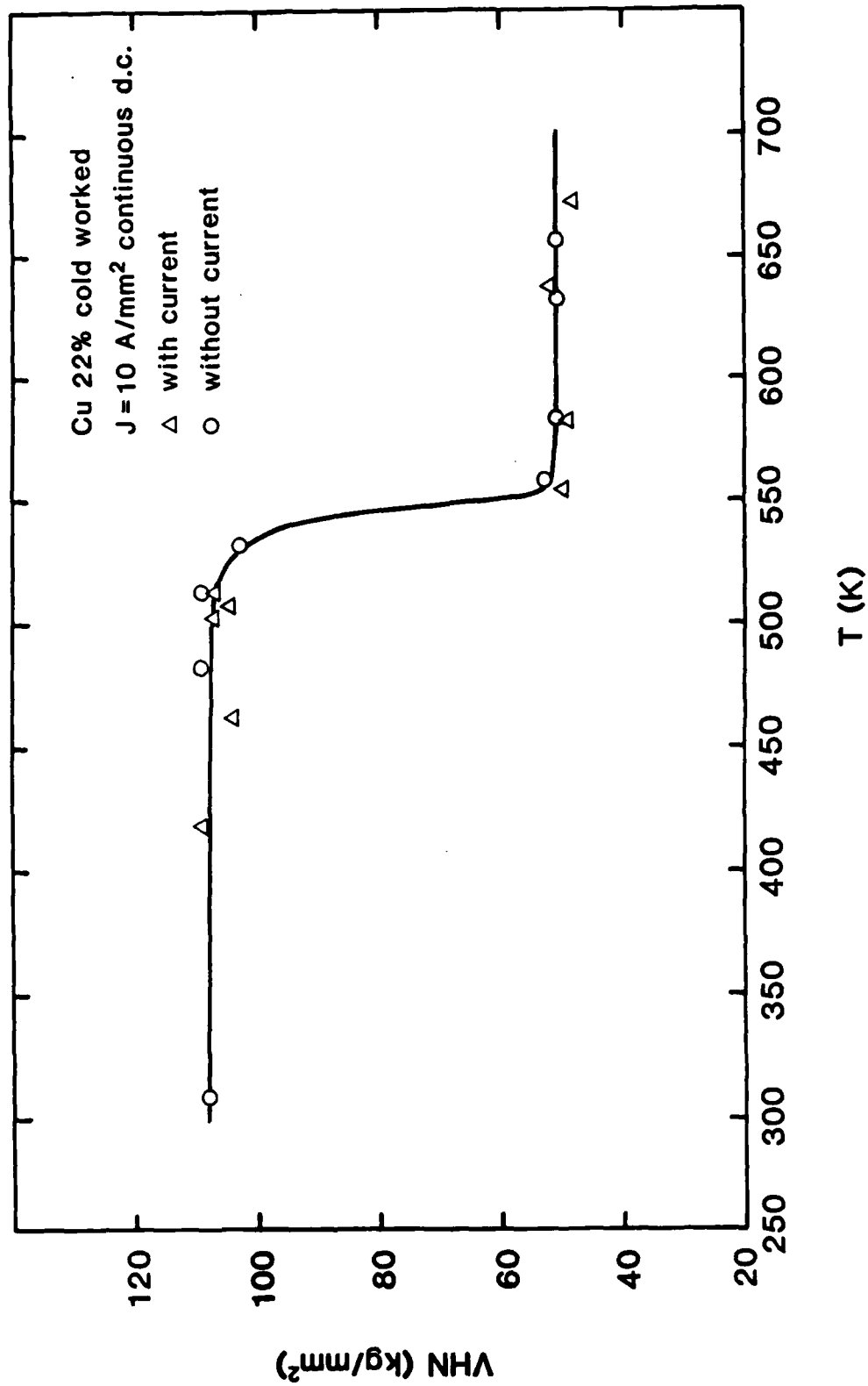

Fig. 18 Effect of continuous d.c. current of 10 A/mm^2 on the annealing behavior of Cu cold worked 22%.

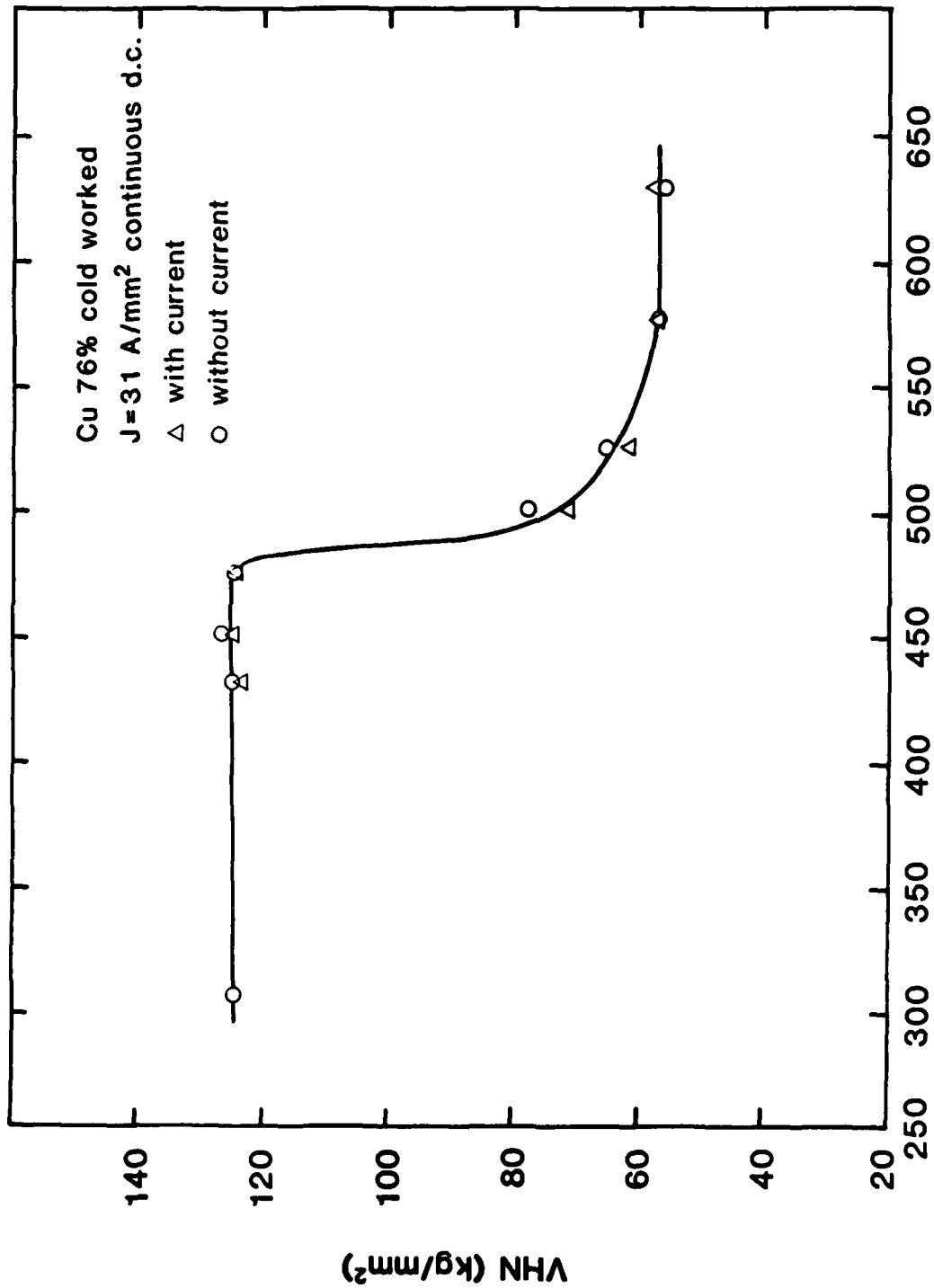

Fig. 19 Effect of a continuous d.c. current of 31 A/mm^2 on the annealing behavior of Cu cold worked 76%.

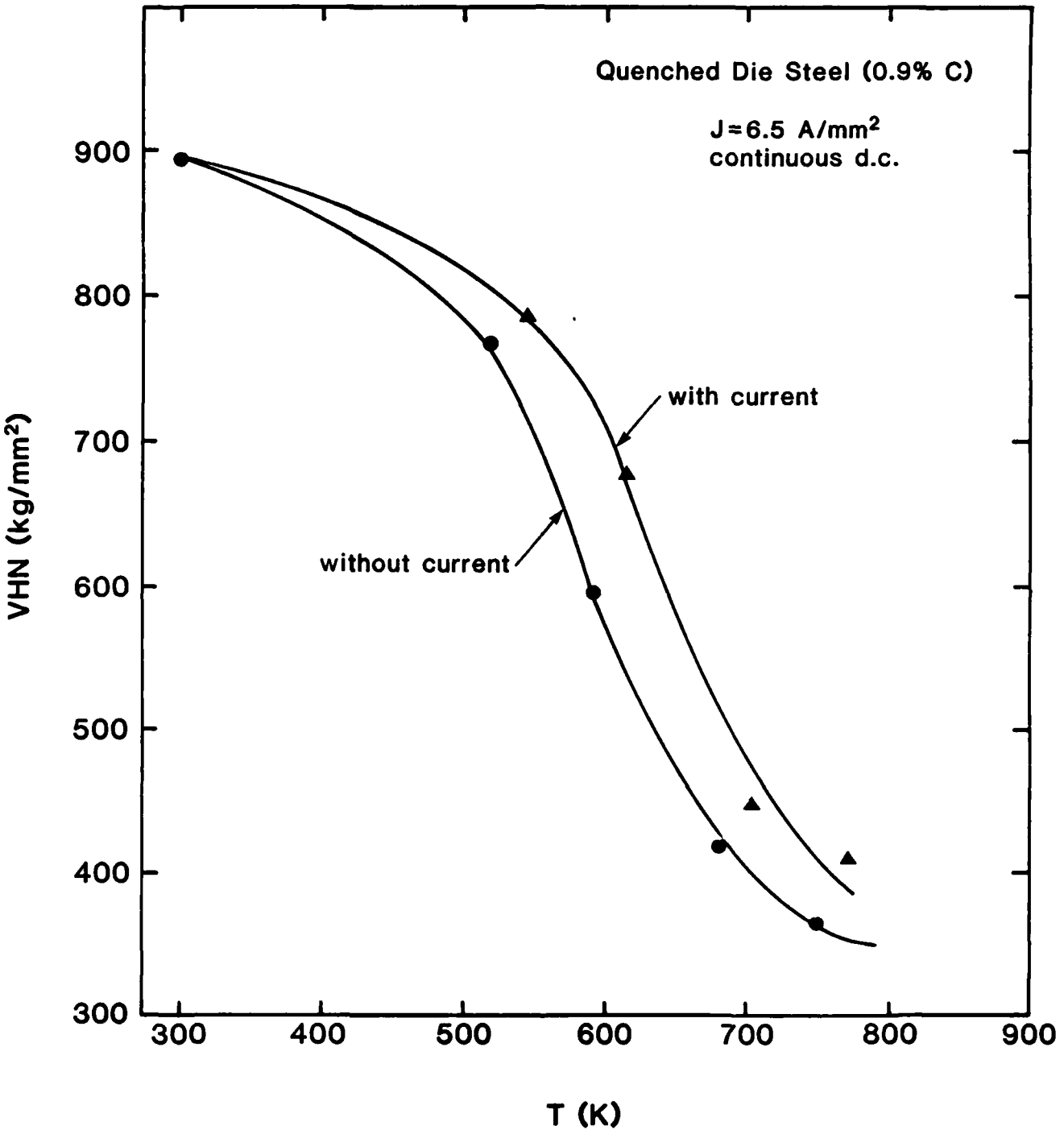

Fig. 20 Effect of a continuous d.c. current of 6.5 A/mm^2 on the tempering (t = 1/2 hr) of a hardened AISI (02) tool steel.

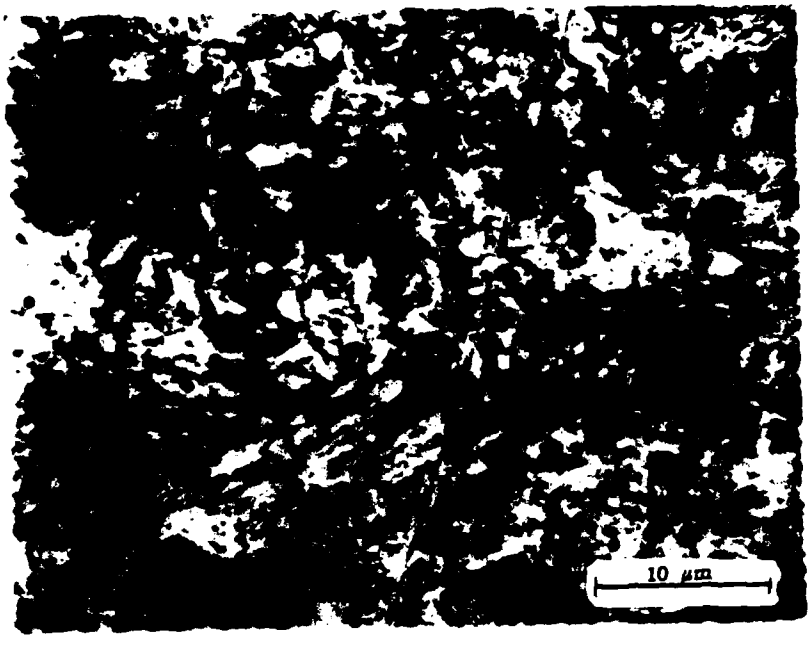

(a)

(b)

Fig. 21 Effect of a continuous d.c. current of 6.5 A/mm^2 on the microstructure of a hardened AISI (02) tool steel tempered for the fixed time and temperature of 30 min at ~ 600K: (a) J = 6.5 A/mm^2, 611K and (b) no current, 591K.

(a)

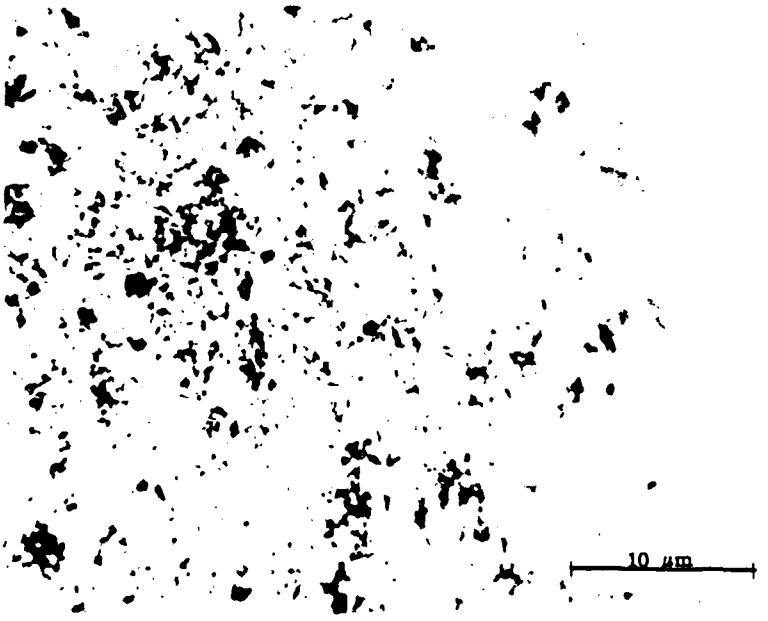

(b)

Fig. 22 Effect of a continuous d.c. current of 6.5 A/mm^2 on the microstructure of a hardened AISI (02) tool steel tempered to a constant hardness of ~ 410 VHN: (a) 30 min at 787K with J = 6.5 A/mm^2 and (b) 30 min at 679K with no current.

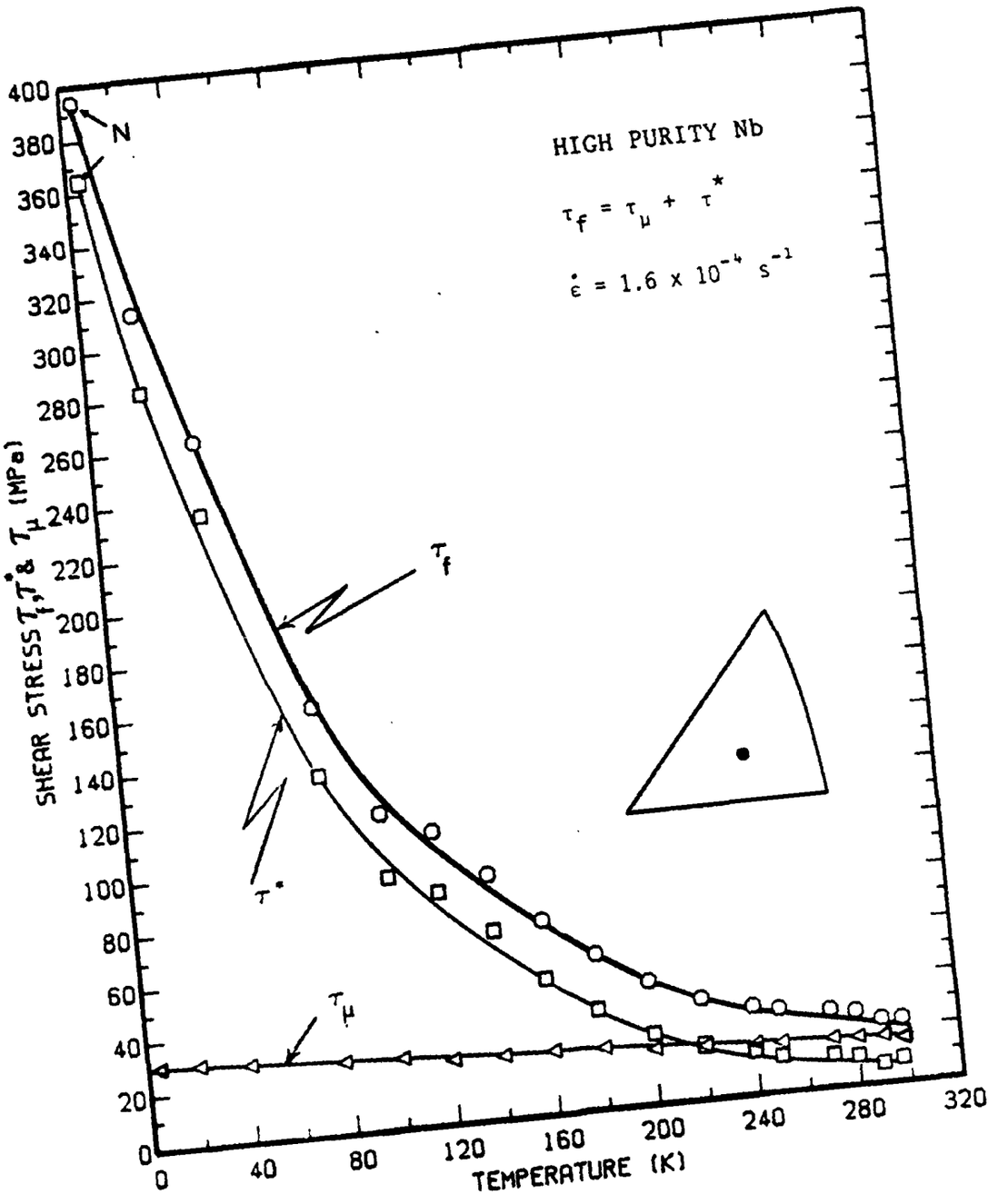

Fig. 23 Effect of temperature on the yield stress (τ_f) and on the thermal and athermal components of the flow stress (τ^* and τ_μ) for Nb single crystals. Letter N at 4.2K indicates test was conducted in the "normal state" obtained by application of a magnetic field.

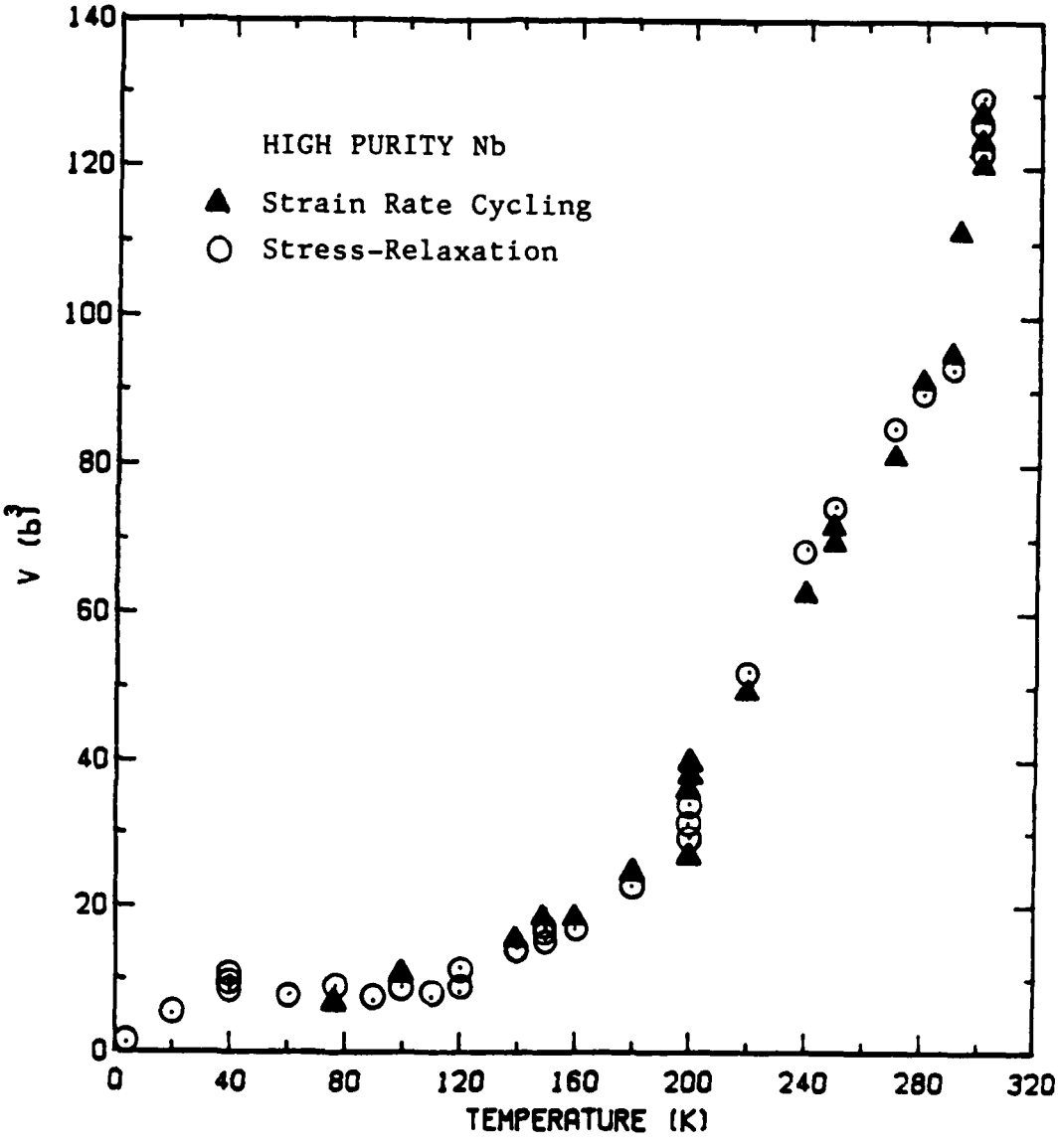

Fig. 24 Variation of the activation volume $v = kT\partial \ln \dot{\gamma}/\partial \tau$ with temperature for Nb single crystals from strain rate cycling and stress relaxation tests.

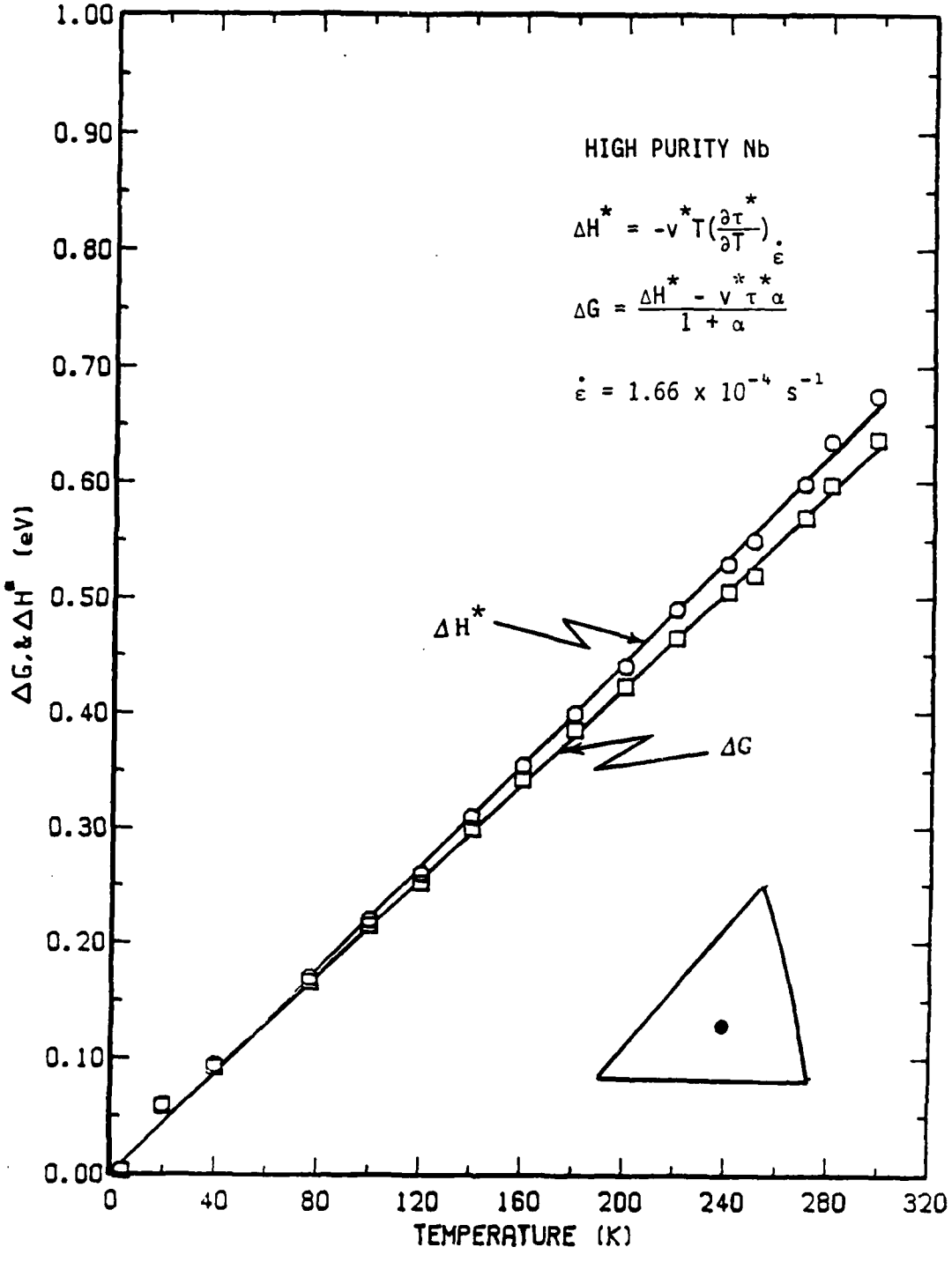

Fig. 25 Variation of the activation enthalpy ΔH^* and the Gibbs free energy of activation ΔG with temperature for the plastic deformation of Nb single crystals at a tensile strain rate of $1.66 \times 10^{-4}\ s^{-1}$.

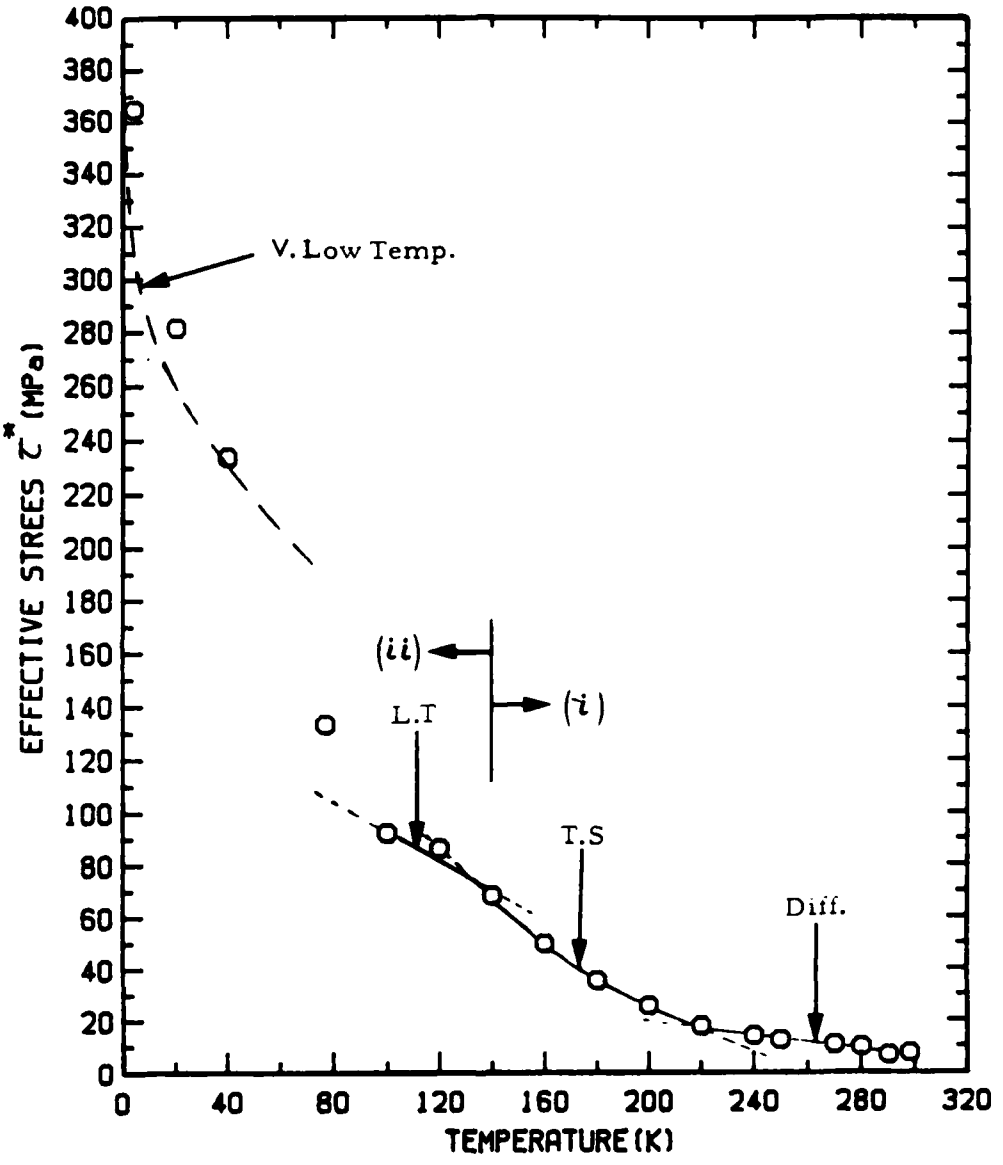

Fig. 26 The temperature dependence of τ^* showing the different approximations in Seeger's model (117, 125).

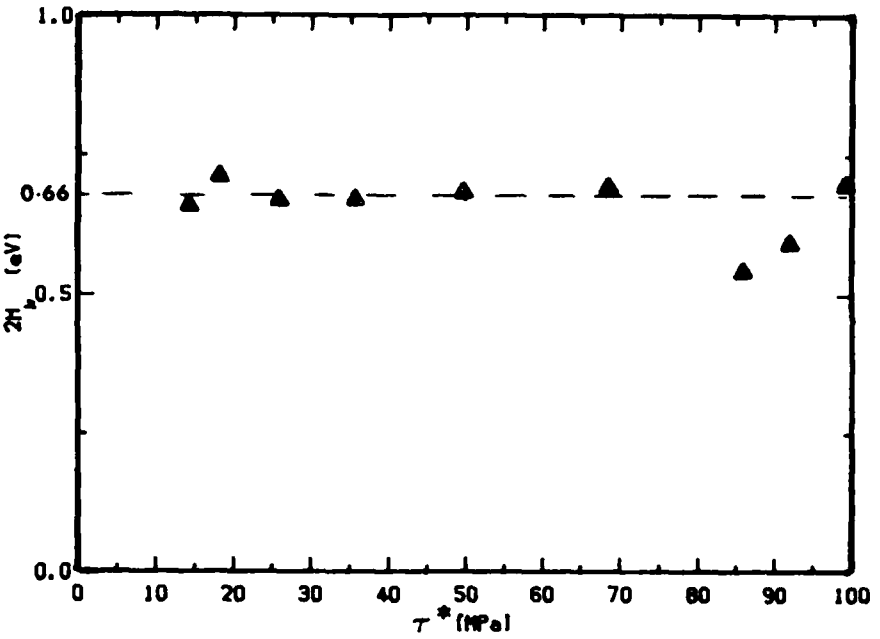

Fig. 28 Values of $2H_k$ derived using the transition state approximation at various stress levels.

END

FILMED

3-86

DTIC